Electron acceptors of the fluorene series. Part 5.[1] Intramolecular charge transfer in nitro-substituted 9-(aminomethylene)fluorenes

Igor F. Perepichka,*[a] Anatolii F. Popov,[a] Tatyana V. Orekhova,[a] Martin R. Bryce,*[b] Alexander N. Vdovichenko,[a] Andrei S. Batsanov,[b] Leonid M. Goldenberg,†[b,c] Judith A. K. Howard,[b] Nikolai I. Sokolov[d] and (in part) Joanne L. Megson[b]

[a] *Institute of Physical Organic & Coal Chemistry, National Academy of Sciences of Ukraine, Donetsk 340114, Ukraine*
[b] *Department of Chemistry, University of Durham, Durham, UK DH1 3LE*
[c] *School of Engineering, University of Durham, Durham, UK DH1 3LE*
[d] *Laboratory of Holography, Natural Faculty, University 'Kievo-Mogilyanskaya Academy', Kiev 254145, Ukraine*

Strong intramolecular charge transfer (ICT) in fluorenes 2 and 3 from a donor amino group to acceptor fluorene moiety leads to exceptionally easy rotation around the C(9)=C(α) bond that has been registered by ^{1}H NMR spectroscopy; single crystal X-ray analysis of 2i confirms the changes in the bond numbers. Cyclic voltammetry (CV) of compounds 2 and 3 shows two closely spaced reversible single-electron reduction waves (in the range of −0.4 V to −1.16 V, $E_{1red}^{\frac{1}{2}} - E_{2red}^{\frac{1}{2}} \leqslant 0.16$ V) resulting in radical anions and dianions, respectively, and a third reduction wave [$E_{3red}^{\frac{1}{2}} \approx -(1.31 - 1.53)$ V] resulting in radical trianions. $E_{3red}^{\frac{1}{2}}$ shows very little dependence on the structure of compounds 2 and 3, whereas $E_{1red}^{\frac{1}{2}}$ and $E_{2red}^{\frac{1}{2}}$ correlate well with σ_p^- constants of substituents in the fluorene ring. At +0.71 V to +1.55 V a single-electron oxidation wave yielding radical cations of the compounds 2 and 3 is observed in CV. Parameters ρ_{CV}^- for reduction ($E_{1red}^{\frac{1}{2}}$ and $E_{2red}^{\frac{1}{2}}$) and oxidation ($E_{ox}^{\frac{1}{2}}$) of compounds 2 and 3 are in the region of 0.12 V to 0.20 V. The influence of the structure and solvent effects on the ICT energies have been studied by UV–VIS spectroscopy. It has been found that the ICT energies also correlate well with σ_p^- constants in the fluorene ring; however, in contrast to CV investigations which demonstrated close ρ_{CV}^- values for both series of the compounds [ρ_{1red}^- (2) = 0.195 ± 0.005 V ≈ ρ_{1red}^- (3) = 0.175 ± 0.005 V, in acetonitrile], the sensitivity parameter ρ_{ICT}^- for 2 is approximately twice that for 3 (−0.175 ± 0.008 eV and −0.085 ± 0.008 eV, respectively, in acetonitrile). A quantitative estimation of solvent effects on the ICT energies using the four-parameter Koppel–Palm equation shows that only polarity and basicity of the solvent are statistically relevant in all the cases. Spectroelectrochemical studies on the compound 2i show the disappearance of the ICT band in the visible spectra when the negative potential yielding the radical anion and/or the dianion is applied. An increased electrophotographic sensitivity of poly-*N*-(2,3-epoxypropyl)carbazole (PEPC) films sensitized by compound 2d has been found in the ICT region; this phenomenon can be used for elaboration of photothermoplastic films with selective regions of the photosensitivity.

Introduction

Electron acceptors of the fluorene series are gaining attention in the study of intermolecular charge-transfer complexes which possess specific electro-physical properties, as electron transport materials and as photoconductivity sensitizers for carbazole-containing polymers.[2] It has been shown[3] that semiconductive polymers containing, as sensitizers, electron acceptors of the fluorene series with intramolecular charge transfer (ICT) may exhibit increased photoconductivity in the ICT region of the acceptor. Therefore, a study of the influence of the structure of fluorene compounds containing both acceptor and donor moieties upon ICT energies is of considerable interest.

Strong electron acceptors having a dicyanomethylene fragment, *e.g.* 7,7,8,8-tetracyano-*p*-quinodimethane (TCNQ, E_A = 2.88 eV) and tetracyanoethylene (TCNE, E_A = 2.75 eV),[4] react with aliphatic amines with substitution of one or two cyano groups by amino groups depending upon the molar ratio of amine used.[5] It is known that similar cyano group substitution occurs for the strongest electron acceptor of the fluorene series, *i.e.* 9-dicyanomethylene-2,4,5,7-tetranitrofluorene (**1i**, E_A = 2.62 eV,[6] 2.75 eV[1b]).

However, in this case the substrate is a more complicated system (as compared to TCNE and TCNQ) and generally different sites for the nucleophilic attack are possible (Fig. 1). Some of the reactions of this type have been described in the literature, *e.g.* substitution of nitro groups in polynitrofluoren-9-ones by the reaction of amines (at position 2),[7] hydroxide ion (at positions 2 and 4),[8] thiophenolate ion (at position 4),[9] butanethiolate ion (at positions 2 and 7)[10] and by nucleophilic addition of cyanide ion at position 9 of 9-dicyanomethylenefluorene with the formation of 9-cyano-9-dicyanomethylfluorene.[11] Additionally, 9-dicyanomethylenenitrofluorene derivatives, being strong electron acceptors, are able to form radical-ion salts with the aliphatic amines acting as donors.[12]

We have found that 9-dicyanomethylenenitrofluorene derivatives (**1a–h**), with lower electron affinity values, react with secondary amines with subsequent substitution of cyano groups by amino groups, similar to acceptor **1i**, although in lower yields, giving derivatives of 9-[cyano(dialkylamino)methyl-

† On leave from the Institute of Chemical Physics in Chernogolovka, Russian Academy of Sciences, Chernogolovka, Moscow Region 142432, Russian Federation.

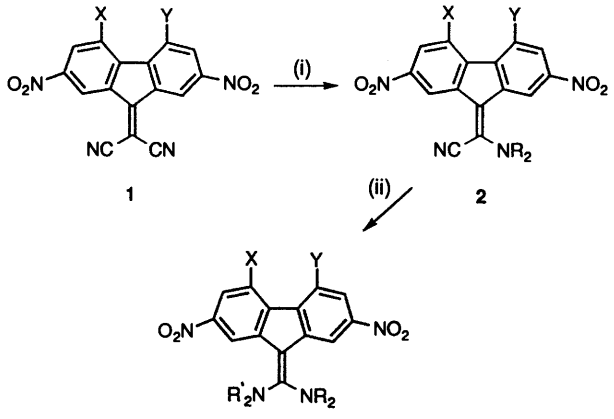

a	X = Y = H		R = R' = Me
b	X = H	Y = C(O)NMe$_2$	R = R' = Me
c	X = H	Y = COOMe	R = R' = Me
d	X = H	Y = COOBu	R = R' = Me
e	X = H	Y = CN	R = R' = Me
f	X = H	X = NO$_2$	R = R' = Me
g	X = NO$_2$	Y = COOMe	R = R' = Me
h	X = NO$_2$	Y = C(O)N(C$_{10}$H$_{21}$)$_2$	R = R' = Me
i	X = Y = NO$_2$		R = R' = Me
j	X = H	Y = NO$_2$	R = R' = -(CH$_2$)$_5$-
k	X = H	Y = NO$_2$	R = R' = -(CH$_2$)$_2$-O-(CH$_2$)$_2$-
l	X = NO$_2$	Y = C(O)NHC$_{10}$H$_{21}$	R = R' = -(CH$_2$)$_2$-O-(CH$_2$)$_2$-
m	X = H	Y = NO$_2$	R = Me; R' = -(CH$_2$)$_2$-O-(CH$_2$)$_2$-
n	X = Y = NO$_2$		R = Me; R' = -(CH$_2$)$_5$

Scheme 1 *Reagents and conditions:* (i) R_2NH (1.0–1.1 equiv.), 25 °C, 1–6 h (monitored by TLC); (ii) R'_2NH (3–9 equiv.), 25–56 °C, 30 min–2 days (monitored by TLC)

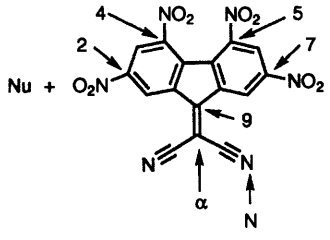

Fig. 1 Possible sites of nucleophilic attack in the fluorene acceptor **1i**

ene]fluorenes (**2**) and 9-[bis(dialkylamino)methylene]fluorenes (**3**), (Scheme 1). We also now report results of investigations of ICT in the above compounds **2** and **3** by ^{1}H NMR and UV–VIS spectroscopy in solution and, in the solid state, by single crystal X-ray diffraction structural analysis; cyclic voltammetry studies of reduction/oxidation of the above compounds, spectroelectrochemical data and sensitization of photoconductivity of PEPC are also reported.

Results and discussion

Synthesis

The synthesis of compounds **2** and **3** is presented in Scheme 1. Substitution of the first cyano group in compounds **1a–i** proceeds smoothly at room temperature in such solvents as dioxane, acetonitrile and acetone with the molar ratio of reagents **1a–i**: amine, 1 : (1.0–1.1). Depending on the substituent in the fluorene nucleus, the reaction requires from 10 to 15 min for **1i** and up to 3 to 5 h for **1a**. For substitution of the second cyano group, a 3–9 fold excess of amine was used and the reaction was carried out with heating (50–80 °C) for between 10 min and up to several hours, or at room temperature for up to 2

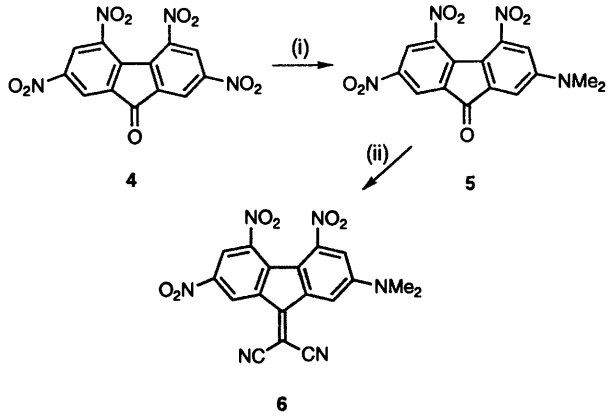

Scheme 2 *Reagents and conditions:* (i) 33% aq. Me_2NH, acetonitrile, 80 °C, 30 min; (ii) $CH_2(CN)_2$, DMF, 60 °C, 2 h

days. The target products were isolated and purified, as a rule, by column chromatography on silica gel.

The synthesized compounds **2** and **3** are high-melting intensely coloured crystalline products (red colouring for **2** and dark violet for **3**). The presence of the electron donating substituent (R_2N) and the acceptor fluorene fragment in molecules **2** and **3** results in ICT which is manifested in the appearance of an additional absorption band in the visible region (*i.e.* ICT band) in the electronic absorption spectra (see below), which causes their colouring.

The synthesis conditions, yields and characteristics for products **2** and **3** are given in Table 1. It should be noted that the substitution rates for the first and second cyano groups (reactions **1** ⟶ **2** and **2** ⟶ **3**) differ substantially (by about 10 to 30 times) permitting isolation of mono- or di-substitution products, depending on the reaction conditions (the ratio of amine–acceptor, time and temperature). The drop in reactivity when substituting the electron withdrawing cyano group by a donating dialkylamino-substituent is to be expected in nucleophilic substitution reactions at a C=C double bond.[13]

A reduction in the electron-accepting nature of the fluorene fragment in compounds **1** upon changing the substituents X and Y also results in a decrease in the rate of the substitution reaction. Additionally, the yields of products **2** and **3** decrease due to increased contribution of the reactions occurring at other sites, as shown in Fig. 1. Thus, among the reaction products, the corresponding fluoren-9-ones have been identified, probably formed by hydrolysis of the corresponding imminium salts (the products of the amine attack at position 9 of compounds **1**) or as a result of the attack of the hydroxide ion (formed upon equilibrium in the reaction of amine with water contained in the solvent, or when 33% aqueous dimethylamine was used).

In a previous paper[6] it was mentioned that no substitution of the nitro groups was observed in the interaction of compound **1i** with secondary amines. To verify this statement we performed an alternative synthesis of compound **6** (Scheme 2). Substitution of a nitro group in 2,4,5,7-tetranitrofluoren-9-one (**4**) by the dimethylamino group occurs at position 2, similar to the reaction with piperidine described earlier;[7] condensation of compound **5** with malononitrile in DMF yielded compound **6**. In compounds **5** and **6** an intense ICT from the donor dimethylamino substituent to the acceptor fluorene fragment is also observed. TLC-monitoring of the reaction mixture during the synthesis of compounds **2i** and **3i** from **1i** indicated the presence of trace quantities of compound **6**, *i.e.* the formation of compounds of type **6** may be a minor reaction route.

Substitution of the cyano groups in 2-nitro-9-dicyanomethylenefluorene was not observed even upon its heating in DMF at

Table 1 Reaction conditions, yields, melting points, elemental analysis and UV–VIS spectral data for substituted 9-(aminomethylene)fluorenes **2** and **3**

Compound	X	Y	R,R'[a]	Reaction conditions[b]	Yield (%)[c]	Mp/°C[d]	Found (%)			Empirical formula	Requires (%)			λ_{max}/nm[e] (ε/dm^3 mol^{-1} cm^{-1})
							C	H	N		C	H	N	
2a	H	H	Me	AN, 30 °C, 5–6 h	14	299–300 (acetone)	60.55	3.70	16.75	$C_{17}H_{12}N_4O_4$	60.7	3.6	16.65	—
2b	H	$CONMe_2$	Me	AN, 30 °C, 2 h	26	287–288 (acetone)	58.6	4.3	17.05	$C_{20}H_{21}N_5O_5$	58.95	4.2	17.2	258 (28 000), 317 (16 920), 347 (16 430), 464.1 (11 650)
2c	H	COOMe	Me	AN, 30 °C, 1 h	29 (LC:B)	246.5–247.5	57.7	3.6	14.25	$C_{19}H_{14}N_4O_6$	57.85	3.6	14.2	256 (26 020), 281 (17 760), 310 (16 930), 350.5 (17 020), 470.7 (11 190)
2d	H	COOBu	Me	AN, 30 °C, 1 h	24 (LC:B)	163–164 (ethanol)	60.35	4.6	12.75	$C_{22}H_{20}N_4O_6$	60.55	4.6	12.85	256 (23 060), 281.5 (15 670), 310.5 (15 080), 350 (14 900), 471.1 (9710)
2e	H	CN	Me	Dioxane, 100 °C, 2 h	24 (LC:B)	303–306	59.9	3.15	19.45	$C_{18}H_{11}N_5O_4$	59.8	3.05	19.35	—
2f	H	NO_2	Me	AN, 30 °C, 2 h	35	270–273 (AN)	53.65	2.85	18.50	$C_{17}H_{11}N_5O_6$	53.55	2.9	18.35	255 (28 100), 276sh (20 700), 353 (16 990), 426 (9970), 488.4 (11 650)
2g	NO_2	COOMe	Me	Dioxane, 30 °C, 5 h	36 (LC:B)	249–252	52.05	3.0	15.95	$C_{19}H_{13}N_5O_8$	51.95	3.0	15.95	252 (21 090), 287 (15 280), 362 (13 400), 425 (10 240), 513.8 (10 660)
2h	NO_2	$CON(C_{10}H_{21})_2$	Me	AN, 30 °C, 4 h	32 (LC:B)	177–179	64.95	7.65	11.85	$C_{38}H_{52}N_8O_7$	64.75	7.45	11.9	—
2i	NO_2	NO_2	Me	AN, 30 °C, 1 h	38 (LC:B–A)	296–298 (chlorobenzene)	48.1	2.4	19.45	$C_{17}H_{10}N_6O_8$	47.9	2.35	19.7	253.3 (27 360), 280sh (16 000), 351.6 (14 300), 436.8 (9550), 531.2 (9700)
2j	H	NO_2	$-(CH_2)_5-$	AN, 30 °C, 1 h	39	257–258 (dioxane)	57.05	3.6	16.75	$C_{20}H_{15}N_5O_6$	57.0	3.6	16.65	—
2k	H	NO_2	$-(CH_2)_2-O-(CH_2)_2-$	AN, 30 °C, 2 h	23	244–246 (AN)	53.8	3.1	16.8	$C_{19}H_{13}N_5O_7$	53.9	3.1	16.55	—
2l	NO_2	$CONHC_{10}H_{21}$	$-(CH_2)_2-O-(CH_2)_2-$	Dioxane, 30 °C, 1 h	27 (LC:B–A)	233–238 (AN:propan-2-ol, 1:3)	59.6	5.7	13.95	$C_{30}H_{34}N_6O_8$	59.4	5.65	13.85	—
3a	H	H	Me	AN, 25 °C, 48 h, (1:9)	15 (LC:B)	227–230	60.95	5.05	15.8	$C_{18}H_{18}N_4O_4$	61.0	5.1	15.8	223.5 (32 490), 258 (15 300), 298 (36 740), 369 (45 650), 547.0 (3290)
3b	H	$CONMe_2$	Me	AN, 25 °C, 24 h, (1:4)	25 (LC:B–A)	258–262	57.55	5.0	15.95	$C_{21}H_{23}N_5O_5$	57.4	5.05	15.95	223 (28 550), 255sh (15 000), 302.5 (34 610), 369.5 (40 180), 550.7 (3490)
3c	H	COOMe	Me	AN, 25 °C, 24 h, (1:7)	27 (LC:B)	260–261	58.1	4.85	13.6	$C_{20}H_{20}N_4O_6$	58.25	4.9	13.6	222 (27 740), 303.5 (29 630), 373.2 (38 420), 561.8 (3510)
3d	H	COOBu	Me	AN, 50 °C, 2 h, (1:3)	42 (LC:B)	183–184	60.8	5.8	12.4	$C_{23}H_{26}N_4O_6$	60.8	5.75	12.35	221.5 (26 850), 303.5 (28 330), 373.5 (37 060), 560.2 (3440)
3e	H	CN	Me	Dioxane, 25 °C, 24 h, (1:8)	23 (LC:B)	322–324	60.1	4.6	18.5	$C_{19}H_{17}N_5O_4$	60.15	4.5	18.45	221.5 (30 460), 260 (14 280), 305 (28 480), 330 (25 990), 369 (36 270), 559.5 (3420)
3f	H	NO_2	Me	Dioxane, 25 °C, 24 h, (1:6)	30	294–296 (dioxane)	54.1	4.25	17.55	$C_{18}H_{17}N_5O_6$	54.15	4.3	17.55	300.5 (29 850), 359.5 (33 900), 575.7 (3350)
3g	NO_2	COOMe	Me	Dioxane, 25 °C, 8 h, (1:4.5)	44 (LC:B–A)	278–280 (toluene)	52.45	4.3	15.3	$C_{20}H_{21}N_5O_8$	52.5	4.2	15.3	242 (24 360), 342.5 (29 190), 383.5 (25 380), 591.3 (3800)
3i	NO_2	NO_2	Me	AN, 30 °C, 1 h, (1:3)	40	> 360 (AN)	48.7	3.7	18.8	$C_{18}H_{16}N_6O_8$	48.65	3.65	18.9	246 (22 530), 286.5 (23 070), 338 (27 780), 368.5 (25 230), 602.4 (3580)
3j	H	NO_2	$-(CH_2)_5-$	Acetone, bp, 10 min, (1:4.5)	24	304.5–306.5 (dioxane)	60.25	5.4	14.85	$C_{24}H_{25}N_5O_6$	60.1	5.25	14.6	258 (18 210), 302 (26 480), 371 (35 560), 585.8 (3390)
3k	H	NO_2	$-(CH_2)_2-O-(CH_2)_2-$	AN, bp, 30 min, (1:5)	49	> 360 (AN)	54.8	4.3	14.6	$C_{22}H_{21}N_5O_8$	54.65	4.4	14.5	260sh (17 900), 299 (26 340), 371 (37 010), 566.9 (3620)
3m	H	NO_2	Me $-(CH_2)_2-O-(CH_2)_2-$	AN, 30 °C, 2 h, (1:5)	85	242–244 (acetone)	54.25	4.5	15.65	$C_{20}H_{19}N_5O_7$	54.4	4.35	15.85	257.5 (16 550), 299.5 (26 570), 365.5 (34 290), 572.1 (3420)
3n	NO_2	NO_2	Me $-(CH_2)_5-$											285 (21 900), 340.5 (19 900), 378.5 (19 000), 610.5 (3230)

[a] In all the cases, except compounds **3m** and **3n**, R = R'. [b] Indicated: solvent (AN is acetonitrile), temperature, time and molar ratio. [c] Isolated yield, *i.e.* after purification by liquid column chromatography (LC) where indicated or by recrystallization; B is benzene; B–A is benzene–acetone mixture, 6:1 (v/v). [d] Where applicable the solvent for recrystallization is indicated in parentheses. [e] In acetonitrile, 25 °C.

80 °C for 10 h; refluxing for 2 days yielded a complicated mixture of products.

Kinetics

In contrast to the reaction of compounds **1** with amines which led to compounds **2** in relatively low yields (15–40%, see Table 1) due to many side reactions, the reaction of pure compounds **2** with amines gave the products **3** in near quantitative yields (the compound **3m** was isolated in 85% yield after recrystallization, Table 1). This allowed an investigation of the kinetics of the reaction.

We studied the reaction rate of compound **2i** with piperidine in acetonitrile by the decrease in the optical density of **2i** at three different wavelengths (253, 435 and 527 nm). Spectral changes in the UV–VIS absorption spectra during the reaction **2i** ⟶ **3n** are demonstrated in Fig. 2.

Variations in the piperidine concentrations showed that the reaction is not a simple bimolecular process, but is catalysed by a second molecule of the initial amine and the observed second-order rate constant, k_{obs}/dm^3 mol^{-1} s^{-1}, is a linear function of amine concentration according to eqn. (1), where k_0 and k_B are

$$k_{obs} = k_0 + k_B[B] \quad (1)$$

the rate constants of the non-catalytic route and the route catalysed by a second amine molecule, respectively, and [B] is the concentration of the reacting amine.

This situation often takes place in nucleophilic vinylic substitution reactions of the addition–elimination type (Ad_N–E)[14] with a sluggish leaving group. Thus, with a good leaving group, like Cl or Br, the nucleophilic attack is usually the rate-limiting step and second-order kinetics (first-order in each of the reactants) are observed.‡[15] In the case of a poor leaving group, like F,[16] CN[17,18] or EtO,[17] when the C–X bond cleavage is slow, the first step of the reaction (nucleophilic attack on the double C–C bond) is reversible; deprotonation of the ammonium ion in the zwitterionic intermediate by a second amine molecule precedes the C–X bond cleavage, and base catalysis of the reaction is observed. We believe that just this mechanism is realized for the reaction **2**⟶**3**; such a supposition is in agreement with the observed kinetics of the reaction.

Values of k_{obs} at various piperidine concentrations, and constants k_0 and k_B calculated from eqn. (1) rate are summarized in Table 2. As follows from Table 2, catalytic rate constants, k_B, determined for various wavelengths, are in good agreement (9.93 ± 0.06, 9.85 ± 0.23, and 10.37 ± 0.10 dm^6 mol^{-2} s^{-1} for 253, 435 and 527 nm, respectively). A contribution of the non-catalytic reaction route is very small (k_B/k_0 > 200) or non-existent. Total treatment of the data for k_{obs} at various wavelengths by eqn. (1) gave the catalytic rate constant k_B = 10.21 ± 0.34 dm^6 mol^{-2} s^{-1} and a statistically irrelevant value for k_0 (0.016 ± 0.024 dm^3 mol^{-1} s^{-1}).

^{1}H NMR spectra

For derivatives with an unsymmetrical fluorene fragment (*i.e.* different substituents X and Y) for compound **2** (and for compounds **3** with different amine substituents) two isomers (*i.e.* *Z* and *E*) about the C(9)=C(α)§ bond may exist. Accordingly, ^{1}H NMR spectra of these compounds have been studied. The spectrum for compound **2c** in acetone solution [Fig. 3(*a*)] showed that it exists as a mixture of both isomers with *Z*:*E* ratio close to 50:50. However, the energy of the *Z*–*E* transition is unusually low, so when the sample was heated [Fig. 3(*b*)] and/or a more polar solvent, *e.g.* DMSO, was used [Fig. 3(*c*)–(*e*)], broadening and coalescence of the proton signals of the fluorene ring corresponding to the *Z* and *E* isomers was observed, due to an increased rate of rotation around the formally C(9)=C(α) double bond.

Increasing the number of electron-withdrawing substituents on the ring system also resulted in a lowering of the rotation barrier to the extent that for compounds **2f–i** broadening of the signals of the aromatic protons of the fluorene fragment was observed even at room temperature. Thus, Fig. 4 shows ^{1}H NMR spectra of compound **2i** in acetone. At 50 °C and 18 °C [Fig. 4(*a*) and 4(*b*), respectively] sharp doublet (δ 8.70, $J_{1,3}$ 2.0 Hz) and broad singlet (δ 9.11) peaks for protons H-3,6 and H-1,8, respectively, were observed due to fast rotation (on the NMR timescale) about the C(9)=C(α) bond. Cooling a sample of **2i** resulted in decoalescence of the H-1,8 protons and in coalescence of the H-3,6 protons, and at −90 °C [Fig. 4(*e*)] two sharp doublets (δ 9.50, 8.71, $J_{1,3}$ 2.0 Hz) for H-1 and H-8 and a singlet (δ 8.68) for H-3,6 were observed.

A deceleration in the bond rotation may also be achieved by

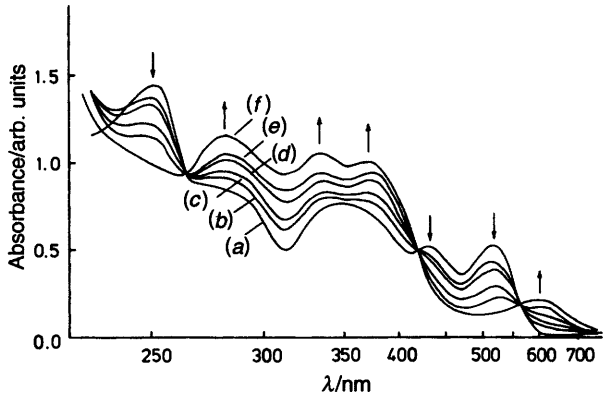

Fig. 2 Changes in the UV–VIS absorption spectra during the reaction **2i** ⟶ **3n** in acetonitrile, 25 °C; [**2i**] = 5.4 × 10^{-5} mol dm^{-3}, [$C_5H_{10}NH$] = 3 × 10^{-3} mol dm^{-3}. Time: (*a*) 0 [starting **2i**]; (*b*) 15 min; (*c*) 30 min; (*d*) 70 min; (*e*) 2 h; (*f*) 19 h.

Table 2 Observed second-order rate constants, k_{obs}, for the reaction of 2,4,5,7-tetranitro-9-[cyano(dimethylamino)methylene]fluorene **2i** with piperidine in acetonitrile at 25 °C at various piperidine concentrations and constants k_0 and k_B calculated from eqn. (1)

[$C_5H_{10}NH$]/10^{-3} mol dm^{-3}	k_{obs}/dm^3 mol^{-1} s^{-1}
	λ = 253 nm
6.50	0.101
13.0	0.166
26.0	0.298
52.0	0.553
	k_0 = (3.73 ± 0.19) × 10^{-2} dm^3 mol^{-1} s^{-1}
	k_B = 9.94 ± 0.06 dm^6 mol^{-2} s^{-1} (*r* 0.9999)
	λ = 435 nm
4.16	0.058
6.73	0.074
8.31	0.0855
13.5	0.123
16.6	0.156
26.9	0.274
33.3	0.324
53.9	0.540
	k_0 = (0.32 ± 1.01) × 10^{-1} dm^3 mol^{-1} s^{-1}
	k_B = 9.85 ± 0.23 dm^6 mol^{-2} s^{-1} (*r* 0.9984)
	λ = 527 nm
7.07	0.108
14.1	0.184
28.3	0.335
56.6	0.622
	k_0 = (3.73 ± 0.38) × 10^{-2} dm^3 mol^{-1} s^{-1}
	k_B = 10.37 ± 0.10 dm^6 mol^{-2} s^{-1} (*r* 0.9999)

‡ Amine catalysis in substrates with Cl as a leaving group, observed in some cases, confirms the multi-step mechanism of the reaction for good leaving groups (refs. 13*c*, 16*a*).

§ In the crystallographic diagram (Fig. 5), C(α) is numbered as C(14).

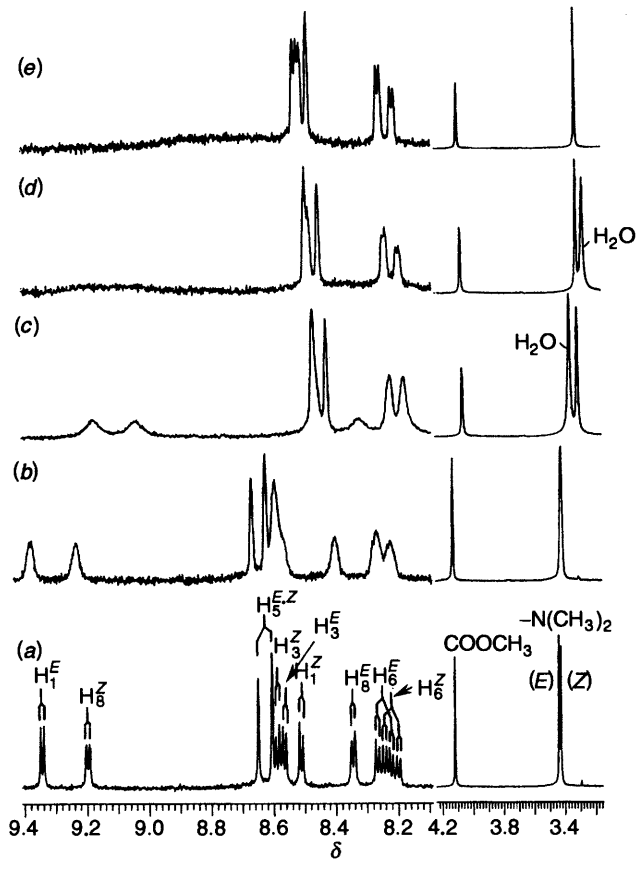

Fig. 3 200 MHz ^{1}H NMR spectra of compound **2c** in [$^2H_6$]acetone at (*a*) 25 °C, (*b*) 50 °C and in [$^2H_6$]DMSO at (*c*) 20 °C, (*d*) 38 °C and (*e*) 90 °C

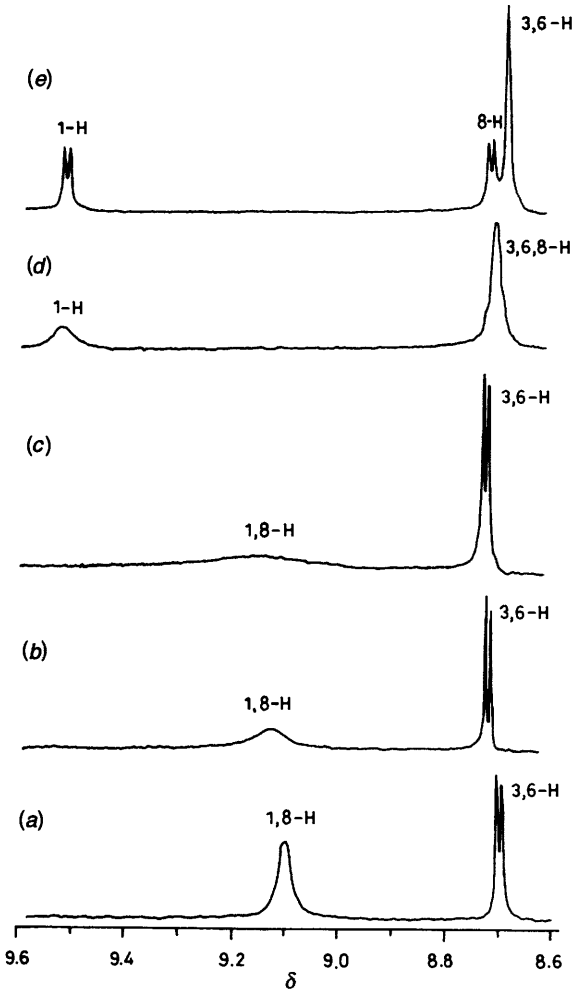

Fig. 4 200 MHz ^{1}H NMR spectra of compound **2i** in [$^2H_6$]acetone at (*a*) 50 °C, (*b*) 18 °C, (*c*) −10 °C, (*d*) −60 °C and (*e*) −90 °C

increasing the steric hindrance in the amine: thus, for trinitro-derivatives of **2** in acetone (20 °C) for R = CH_3 (**2f**) broadened proton signals for H-1,3,6,8 were observed, whereas for R_2N = $(CH_2)_5N$ (**2j**), $O(CH_2CH_2)_2N$ (**2k**) the ^{1}H NMR spectrum displayed sharp signals from the separate *Z* and *E* isomers (for the values of chemical shifts and coupling constants see Table 3). With compounds **3a–f** the rotation barrier around the C(9)=C(α) bond is lowered still further, and time-averaged signals of the *Z* and *E* isomers were observed at all temperatures over the range +25– −70 °C. Moreover, rotation around the C(α)–NR_2 bond became hindered, which results in magnetic inequivalence of the R substituents at one nitrogen atom; thus, for compounds **3** with R = CH_3, two singlets from the methyl groups were observed. With R = R′ the *Z*–*E* transition is degenerate. Using amines with different R and R′ groups (dimethylamine and morpholine) confirmed the correct assignment of these signals (compounds **3f**, **3j** and **3m**, Table 4).

Such behaviour, *i.e.* unusually easy rotation around a C=C double bond in solution, is explained by the pronounced dipolar nature of compounds **2** and **3**, resulting from intramolecular charge transfer from the donor part of the molecule to the acceptor part, represented by resonance structures **7** and **8**, respectively.

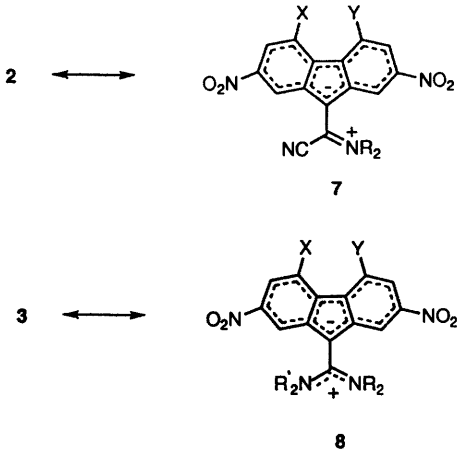

Single crystal X-ray analysis of 2i

To study this process in the solid state the molecular structure of compound **2i** was determined by single crystal X-ray analysis (Fig. 5) which revealed that the exocyclic double bond C(9)=C(14) is conjugated with the lone electron pair of N(2), resulting in significant π-bond delocalization along the C(9)–C(14)–N(2) moiety. The bond distances C(9)–C(14), 1.388(4) Å and C(14)–N(2), 1.342(4) Å (Table 5) correspond to bond orders of 1.55 and 1.40, respectively.[19] The slight twist around these bonds (by 19° and 25°, respectively) and some non-planarity of the bond configuration around N(2) [which deviates from the C(14)–C(16)–C(17) plane by 0.13 Å, the sum of the C–N–C angles being 357.4° (Table 5)] are both consistent with such a description. Similar structural behaviour (change of bonds lengths and near planar sp^2 configuration of the nitrogen atoms of amino groups) has been observed recently for other push–pull compounds, *e.g.* 1,1-dicyano-2,2-bis(dimethylamino)ethylene,[20] and related cumulogues and vinylogues.[21] On the other hand, the C(14)–C(15) distance [1.460(4) Å] in **2i** is slightly longer than the average C(sp^2)–C(sp) single bond lengths in cyanoaryls [1.443(8) Å], TCNQ [1.427(10) Å],[22] H_2C=CH–CN (1.435 Å) or H_2C=CH–C≡CH (1.431 Å),[23] *i.e.* conjugation between the C≡N bond and the p_π-orbital of C(14) is inhibited, as often occurs in the presence of an electronegative atom.[24]

Table 3 ^{1}H NMR chemical shifts (δ_H) and coupling constants (J/Hz) for compounds **2** in [$^2H_6$]acetone (25 °C)[a]

Compound	1-H	3-H ($J_{1,3}$)	5-H ($J_{5,6}$)	6-H	8-H ($J_{6,8}$)	$-N(CH_3)_2$	Other signals
2a	—	—	—	—	—	3.37s	—
2b	—	—	—	—	—	3.43s	3.28 [3 H, s, $-CO-N(CH_3)CH_3$], 2.93 [3 H, s, $-CO-N(CH_3)CH_3$]
2c	*E*: 9.34 d *Z*: 8.51 d	*E*: 8.59 d (2.1) *Z*: 8.57 d (2.1)	*E*–*Z*: 8.63 d (8.8)	*E*: 8.22 dd *Z*: 8.25 dd	*E*: 8.34 d (2.1) *Z*: 9.20 d (2.1)	3.437s[b] 3.424s[b]	4.12 s (3 H, $COOCH_3$)
2f						3.55s	—
2g	broad	8.53 d (2.1)	—	8.68 d (2.0)	broad	3.68s	3.94 (3 H, s, $COOCH_3$)
2h	broad	8.17 d (1.9)	—	8.58 d (2.0)	broad	3.62s	3.4 m, 1.8 m, 1.3 m [36 H, $-(CH_2)_9-$], 0.88 (6 H, m, CH_3)
2i	—	—	—	—	—	3.70s	—
2k	*E*: 9.56 d *Z*: 8.73 d	*E*: 9.01 d (1.9) *Z*: 8.80 d (2.2)	*E*–*Z*: 8.24 d (8.9)	*E*–*Z*: 8.39 dd	*E*: 8.79 d (2.0) *Z*: 9.34 d (2.2)	—	4.05 [4 H, t, *J* 4.6, $N(CH_2CH_2)_2O$], 3.78 [4 H, m, $N(CH_2CH_2)_2O$]

[a] Not all the compounds **2** showed sharp signals of the aromatic protons due to *E*–*Z* isomerization (see text); δ_H are indicated only where observable. [b] Two singlets of methyl groups corresponding to *E* and *Z* isomers were observed at room temperature; heating the sample led to their coalescence.

Table 4 ^{1}H NMR chemical shifts (δ) and coupling constants (J/Hz) for compounds **3** in [$^2H_6$]acetone

Compound	1-H ($J_{1,3}$)	3-H	5-H ($J_{5,6}$)	6-H ($J_{6,8}$)	8-H ($J_{5,8}$)	$-N-CH_3$ CH_3	$-N-CH_3$ CH_3	Other signals
3a	8.11dd (2.2)	7.94dd	8.32dd[a] (8.6)	7.94dd (2.2)	8.11dd (0.5)	3.41s	3.07s	—
3b	4d (2.1)	7.76d	7.99d (8.8)	7.90dd (2.1)	8.14d	3.46s	3.09s	3.29s [3 H, $-CO-N(CH_3)CH_3$], 3.08s [3 H, $-CO-N(CH_3)CH_3$]
3c	8.30d (2.0)	8.34d	8.78d (9.2)	7.90dd (2.1)	8.15d	3.49s	3.08s	4.12s (3 H, $COOCH_3$)
3d	8.30 broad	8.30 broad	8.77d (9.0)	7.90dd	8.14 broad	3.49s	3.08s	4.56t (2 H, *J* 6.6, $-CO-CH_2-C_3H_7$), 1.89m (2 H, $-COCH_2-CH_2-C_2H_5$), 1.54m (2 H, $-COCH_2CH_2-CH_2-CH_3$), 1.02t (3 H, *J* 7.3, $-COCH_2CH_2CH_2-CH_3$)
3e	8.30d (2.1)	8.41d	8.81dd (8.8)	8.06dd (2.2)	8.23dd (0.6)	3.59s	3.10s	—
3f	8.39d (2.0)	8.44d	8.35d (9.0)	7.95dd (2.2)	8.22d	3.56s	3.10s	—
3g	8.26d (2.2)	8.41d	—	8.50d (2.0)	8.38d	3.60s	3.11s	3.90s (3 H, $COOCH_3$)
3i	8.43d (2.0)	8.61d	—	8.61d (2.0)	8.43d	3.66s	3.13s	—
3j	8.69d (2.1)	8.40d	8.36dd (9.1)	7.94dd (2.3)	8.46dd (0.6)	—	—	3.98 m, 1.86 m, 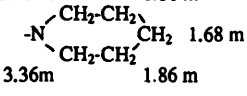 1.68 m, 3.36m, 1.86 m
3k	8.82d (2.0)	8.42d	8.34dd (9.1)	7.97dd (2.3)	8.58dd (0.5)	—	—	3.80 t (*J* 4.4), 4.12 m (broad), 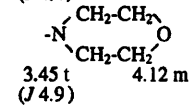 3.45 t (*J* 4.9), 4.12 m (broad)
3m	8.61d (2.0)	8.40d	8.34d (9.1)	7.95dd (2.3)	8.38d	3.64s	3.12	3.80 t (*J* 4.8), 4.12 t (broad) (*J* 5.1), 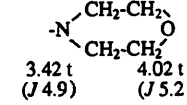 3.42 t (*J* 4.9), 4.02 t (broad) (*J* 5.2)

[a] Chemical shift for protons 4-H and 5-H with an integral intensity of 2 H.

The molecule of **2i** exhibits minor but significant non-planarity in the crystal structure. Rings **A** and **B** adopt sofa and envelope conformations, respectively; in both cases the C(11) atom is bent out of the plane by 0.09 and 0.11 Å, respectively. In ring **C**, the C(5)–C(6)–C(7)–C(8) moiety is planar, with C(12) and C(13) deviating from its plane by 0.12 and 0.09 Å, respectively, in the same direction. The mean planes of the six-membered rings **A** and **C** form a dihedral angle of 12°. This puckering is apparently caused by steric hindrance between the adjacent nitro groups (in positions 4 and 5), which are tilted out of the ring planes in the opposite directions [N(4) and N(5) deviating from these planes by 0.30 Å and −0.33 Å] and rotated around the C–N bonds, thus forming dihedral angles of 34° and 40° with rings **A** and **C**, respectively. Nevertheless, the contacts O(4)···N(5) 2.64 Å, and O(5)···N(4) 2.66 Å between these groups are shorter than the sums of the van der Waals radii (1.40 Å for O, 1.55 Å for N),[25] which can be attributed to electrostatic attraction. For the non-hindered nitro groups in positions 2 and 7, the dihedral angles with rings **A** and **C** are much smaller (20° and 17°, respectively) and the out-of-plane tilting of N(3) and N(6) is insignificant.

These results are consistent with literature data on the

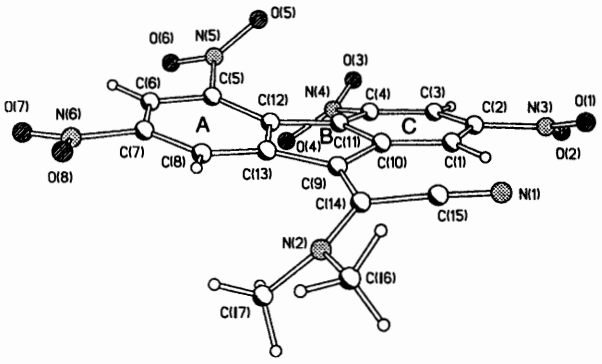

Fig. 5 X-Ray molecular structure of compound **2i**

Table 5 Bond distances (Å) and bond angles (°) in **2i**[a]

O(1)–N(3)	1.219(4)	O(2)–N(3)	1.230(4)
O(3)–N(4)	1.222(4)	O(4)–N(4)	1.234(3)
O(5)–N(5)	1.229(3)	O(6)–N(5)	1.227(3)
O(7)–N(6)	1.236(4)	O(8)–N(6)	1.223(4)
N(1)–C(15)	1.145(4)	N(2)–C(14)	1.342(4)
N(2)–C(16)	1.478(5)	N(2)–C(17)	1.456(4)
N(3)–C(2)	1.478(4)	N(4)–C(4)	1.472(4)
N(5)–C(5)	1.477(4)	N(6)–C(7)	1.481(4)
C(1)–C(2)	1.375(4)	C(1)–C(10)	1.398(4)
C(2)–C(3)	1.384(5)	C(3)–C(4)	1.375(4)
C(4)–C(11)	1.409(4)	C(5)–C(6)	1.378(4)
C(5)–C(12)	1.407(4)	C(6)–C(7)	1.385(5)
C(7)–C(8)	1.374(4)	C(8)–C(13)	1.397(4)
C(9)–C(10)	1.464(4)	C(9)–C(13)	1.455(4)
C(9)–C(14)	1.388(4)	C(10)–C(11)	1.423(4)
C(11)–C(12)	1.459(4)	C(12)–C(13)	1.425(4)
C(14)–C(15)	1.460(4)		
C(14)–N(2)–C(16)	121.1(2)	C(14)–N(2)–C(17)	123.1(3)
C(16)–N(2)–C(17)	113.2(2)	O(1)–N(3)–O(2)	124.7(3)
O(1)–N(3)–C(2)	118.3(3)	O(2)–N(3)–C(2)	117.0(3)
O(3)–N(4)–O(4)	124.6(3)	O(3)–N(4)–C(4)	118.4(3)
O(4)–N(4)–C(4)	116.9(3)	O(5)–N(5)–O(6)	125.4(3)
O(5)–N(5)–C(5)	117.4(2)	O(6)–N(5)–C(5)	117.1(2)
O(7)–N(6)–O(8)	124.4(3)	O(7)–N(6)–C(7)	116.9(3)
O(8)–N(6)–C(7)	118.7(3)	C(2)–C(1)–C(10)	118.3(3)
N(3)–C(2)–C(1)	117.3(3)	N(3)–C(2)–C(3)	119.0(3)
C(1)–C(2)–C(3)	123.6(3)	C(2)–C(3)–C(4)	117.5(3)
N(4)–C(4)–C(3)	115.8(3)	N(4)–C(4)–C(11)	121.2(3)
C(3)–C(4)–C(11)	122.5(3)	N(5)–C(5)–C(6)	115.5(3)
N(5)–C(5)–C(12)	122.5(3)	C(6)–C(5)–C(12)	121.6(3)
C(5)–C(6)–C(7)	118.2(3)	N(6)–C(7)–C(6)	118.3(3)
N(6)–C(7)–C(8)	118.3(3)	C(6)–C(7)–C(8)	123.4(3)
C(7)–C(8)–C(13)	118.1(3)	C(10)–C(9)–C(13)	105.9(2)
C(10)–C(9)–C(14)	126.2(2)	C(13)–C(9)–C(14)	127.7(3)
C(1)–C(10)–C(9)	130.7(3)	C(1)–C(10)–C(11)	120.4(3)
C(9)–C(10)–C(11)	108.9(2)	C(4)–C(11)–C(10)	117.3(3)
C(4)–C(11)–C(12)	134.9(3)	C(10)–C(11)–C(12)	107.7(2)
C(5)–C(12)–C(11)	134.2(3)	C(5)–C(12)–C(13)	117.8(3)
C(11)–C(12)–C(13)	107.6(2)	C(8)–C(13)–C(9)	129.7(3)
C(8)–C(13)–C(12)	120.6(2)	C(9)–C(13)–C(12)	109.3(2)
N(2)–C(14)–C(9)	127.9(2)	N(2)–C(14)–C(15)	113.5(2)
C(9)–C(14)–C(15)	118.5(2)	N(1)–C(15)–C(14)	177.2(3)

[a] For numbering of the atoms, see Fig. 5.

rotation of nitro groups in fluorene derivatives. Thus, a significant rotation of nitro groups attached at positions 4 and 5 was observed for other 4,5-dinitro-substituted fluorenes, *i.e.* 2,4,5,7-tetranitro-9-dicyanomethylenefluorene (**1i**, 35.8° and 34.2°),[26] 2-piperidino-4,5,7-trinitrofluoren-9-one (30.5° and 35.8°),[7] 4,5-dinitrofluoren-9-one (35.5° and 39.3°),[27] 2,4,5-trinitrofluoren-9-one (26.8° and 32.6°),[28] 2,4,5,7- tetranitrofluoren-9-one (for molecules A and B,¶ respectively: 27.4° and 38.6°, 41.4° and 39.0°;[29] 26.4° and 38.7°, 41.7° and 38.9°[30]); for comparison, rotation of the nitro group in the 4 position for 2,4,7-trinitro-9-dicyanomethylenefluorene is smaller (19.3°).[31] The rotations of non-hindered nitro groups in positions 2 and 7 for the above compounds are much smaller (between 7.4° and 16.6°).[7,26–31]

The non-planarity of compound **2i** prevents formation of well-defined stacks in the crystal. However, it is noteworthy that all the molecules in the structure are approximately parallel to the (1 0 2) crystallographic plane (Fig. 6). Each molecule (*e.g.* **I**, see Figs. 6 and 7) contacts on one side with two molecules (**II** and **III**), related to it *via* a 2_1 axis [Fig. 7(*a*)] and on the other side with an inversionally related molecule [**IV**, Fig. 7(*b*)]. In the former case, fused-rings mean planes of the contacting molecules form a dihedral angle of 14°, and in the latter case they are parallel with interplanar separation of *ca.* 3.4 Å. Intermolecular contacts O(4)···C(1) 2.99 and O(4)···C(15) 2.97 Å between molecules **I** and **II**, substantially shorter than the sum of van der Waals radii (3.15 Å),[25] can be attributed to electrostatic interactions, as well as O(8)···N(3) ($x + \frac{1}{2}, y + \frac{1}{2}, z$). More unexpected are the contacts between rotation-related ($-x, y, \frac{3}{2} - z$) molecules, O(2)···O(2') 2.72 Å and O(3)···O(3') 2.84 Å, as due to electrostatic repulsion, O···O distances tend to be longer than double the van der Waals radius of O, estimated from heteroatomic contacts (2.8 Å), and average 3.08 Å for monocoordinate O.[32]

Electrochemistry

Cyclic voltammetry (CV) measurements on the novel compounds **2**, **3**, **5** and **6** were carried out in acetonitrile solution at room temperature with tetraethylammonium tetrafluoroborate as the supporting electrolyte. Measurements were made with Ag/AgCl as the reference electrode using ferrocene as the internal reference (Fig. 8, Table 6).‖

Both series of compounds, *i.e.* **2** and **3**, show similar electrochemical behaviour: two closely-spaced single-electron reduction waves ($\Delta E_{1-2} = E_{1\text{red}}^{\ddagger} - E_{2\text{red}}^{\ddagger} \leqslant 0.16$ V) resulting in radical anion and dianion species, respectively, followed at a considerably more negative potential (0.4–0.8 V more negative) by a third single-electron reduction wave ($E_{3\text{red}}^{\ddagger}$) resulting in the radical trianion. All three waves of the reduction are reversible or quasi-reversible. For compound **2f** the first reduction wave is observed at −0.67 V. The transition from **2f** to **3j** (Fig. 8, Table 6) leads to a shift of the first reduction wave in a more negative direction (−0.93 V) and to some increase in the difference between the first and second reduction potentials (ΔE_{1-2} = 0.08 V for **2f** and 0.12 V for **3j**). Using correlation eqn. (2) describing relationships between electron affinities

$$E_A = (2.59 \pm 0.01) + (1.06 \pm 0.04)\, E_{1\text{red}}^{\ddagger} \qquad (2)$$

(E_A/eV) of acceptors and their first single-electron reduction potentials,[1b] we estimated the electron affinities of the novel acceptors to lie in the ranges 1.65–2.17 eV for compound **2** and 1.36–1.85 eV for compounds **3**, (Table 6) which characterizes them as weak electron acceptors. Differences between E_A values for the corresponding compounds within the series **2** and **3** are in the region of 0.26–0.35 eV.

It is noteworthy that in contrast to strong electron acceptors of the fluorene series (like nitro-derivatives of fluoren-9-one and 9-dicyanomethylenefluorene),[1b] where only the first two reduction waves are reversible followed by multi-electron irreversible reduction of nitro groups, compounds **2** and **3** showed reversible formation of the radical trianion. The potentials of this wave depended much less on the structure of the donor part of the molecule. Thus, the transition from **2f** to **3j**

¶ Two different types of the molecule are observed in the single crystal.[29,30]

‖ Fc^0/Fc^+ couple (Fc = ferrocene) was recommended[33] as the reference redox system for both organic and aqueous media to minimize the contribution from the aqueous–nonaqueous junction potential.

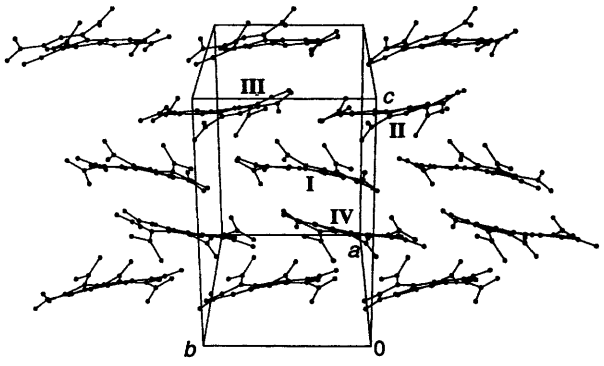

Fig. 6 Crystal packing of compound **2i**, projected on (2 0 −1) plane (H atoms omitted). Labelled molecules are related to the reference one (**I**; x, y, z) by symmetry operations: **II** ($\frac{1}{2} - x, y - \frac{1}{2}, \frac{3}{2} - z$), **III** ($\frac{1}{2} - x, y + \frac{1}{2}, \frac{3}{2} - z$), **IV** ($\frac{1}{2} - x, -\frac{1}{2} - y, 1 - z$).

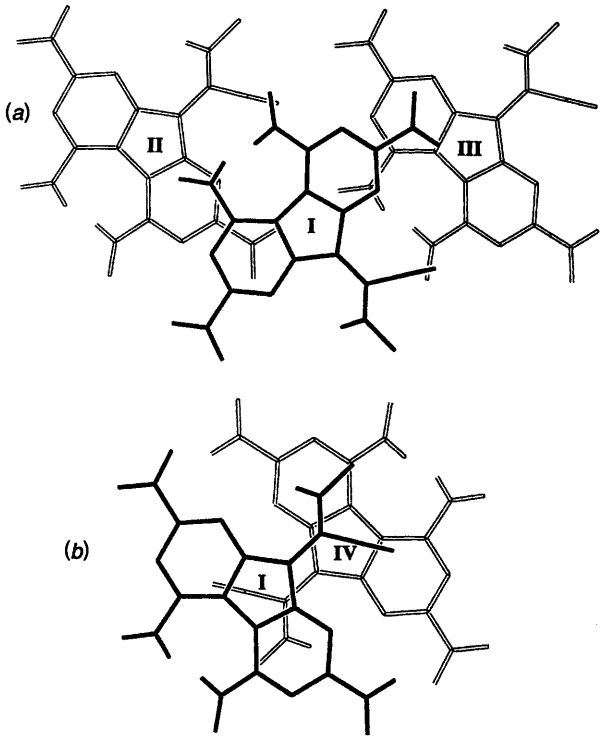

Fig. 7 Molecular overlap in the crystal of **2i**. Projection on (1 0 2) plane; H atoms are omitted; for molecular labelling see Fig. 6

shifted $E_{3red}^{\frac{1}{2}}$ to the negative region by only 0.10 V whereas the first ($E_{1red}^{\frac{1}{2}}$) and second ($E_{2red}^{\frac{1}{2}}$) reduction waves shifted by 0.27 V and 0.30 V, respectively.

Cyclic voltammetry showed also a reversible single-electron oxidation wave ($E_{ox}^{\frac{1}{2}}$) for compounds **2**, **3**, **5** and **6** to yield the radical cation at potentials of between +0.71 and +1.55 V (Fig. 8, Table 6).

It is interesting to note the difference in electrochemical behaviour of compound **6** from that of compounds **2** and **3** indicating that the location of the donor moiety in the fluorene ring exerts a major effect. Compound **6** showed two well-resolved single-electron reduction waves with $\Delta E_{1-2} = E_{1red}^{\frac{1}{2}} - E_{2red}^{\frac{1}{2}} = 0.56$ V which is much greater than that for **2** and **3** (< 0.16 V) and comparable with the ΔE_{1-2} values for polynitrofluoren-9-ones and polynitro-9-dicyanomethylene-fluorenes (*ca.* 0.5–0.6 V).[1b] Compound **6** is a significantly stronger electron acceptor ($E_A = 2.46$ eV, Table 6) in spite of the extremely strong intramolecular charge-transfer interaction, which is greater than that in compounds **2**, **3** and **10** (see below, Electronic absorption spectra section).

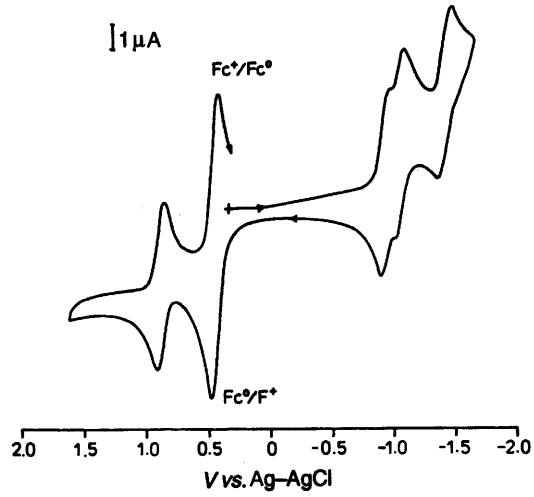

Fig. 8 Cyclic voltammogram of compound **3m**; electrolyte 0.2 M $Et_4N^+BF_4^-$; solvent CH_3CN; scan rate 100 mV s^{-1}; potentials are presented *vs.* Ag/AgCl

For a quantitative estimation of the effect of substituents in compounds **2** and **3** upon their electrochemical behaviour we have used eqn. (3), where $\Sigma\rho_p^-$ is a sum of σ_p^- – nucleophilic

$$E^{\frac{1}{2}} = E_0^{\frac{1}{2}} + \rho^-\Sigma\sigma_p^- \quad (3)$$

constants of the substituents in the fluorene nucleus (X,Y and two nitro groups), $E^{\frac{1}{2}}$ is the half-wave potential of reduction or oxidation of a compound, $E_0^{\frac{1}{2}}$ is $E^{\frac{1}{2}}$ for the reference compound (unsubstituted benzene rings in fluorenes, $\Sigma\sigma_p^- = 0$) and ρ^- is a parameter showing electrochemical potential sensitivity to substituents.

The results are summarized in Table 7. For the reduction processes ($A \longrightarrow A^{\bullet -}$ and $A^{\bullet -} \longrightarrow A^{2-}$) compounds **2** show slightly larger sensitivity of electrochemical potentials to substituents on the benzene rings of the fluorene moiety than compounds **3** [ρ_{1red}^- (**2**) > ρ_{1red}^- (**3**); ρ_{2red}^- (**2**) > ρ_{2red}^- (**3**)], whereas for the oxidation reaction ($A \longrightarrow A^{\bullet +}$) the opposite situation is observed, *i.e.* ρ_{ox}^- (**2**) = 0.120 < ρ_{ox}^- (**3**) = 0.165. The slope of the plots of $E_{red}^{\frac{1}{2}}$ *vs.* $\Sigma\sigma_p^-$ for the first reduction wave ($A \longrightarrow A^{\bullet -}$) is slightly larger than that for second reduction wave ($A^{\bullet -} \longrightarrow A^{2-}$) for both series of compounds, **2** and **3** ($\rho_{1red}^- > \rho_{2red}^-$). Intersection points of these linear dependences (*i.e.* intersection of equations according to entries 2 and 4 for **2**, and 6 and 8 for **3**; Table 7) that correspond to $\Sigma\sigma_p^-$ values at which reduction occurs as a two-electron process with formation of a dianion, are at $\Sigma\sigma_p^- = -2.4$ and +0.6 for **2** and **3**, respectively. These correspond to values at which (and below which) reduction occurs as a two-electron process leading to the formation of the dianion, due to the thermodynamic instability of the radical anion, under the conditions of this investigation.

It is known that the thermodynamic stability of a radical anion can be determined from the difference in potentials of the corresponding radical anion and dianion,[34,35] by the equation $\Delta E_{1-2} = E_{1red}^{\frac{1}{2}} - E_{2red}^{\frac{1}{2}} = -0.059 \log K_{dispr}$, where K_{dispr} is the disproportionation constant in the equilibrium (4).

$$2\,A^{\bullet -} \underset{}{\overset{K_{dispr}}{\rightleftharpoons}} A + A^{2-} \quad (4)$$

Compounds **2** and **3** showed similar thermodynamic stabilities of the radical anions, with K_{dispr} values in the range of 6.5×10^{-2} to 1.9×10^{-3} dm^3 mol^{-1}. In both series of compounds, **2** and **3**, increasing the number of electron withdrawing substituents leads to a decrease in K_{dispr} values

Table 6 Cyclic voltammetry data for fluorene derivatives **2**, **3**, **5** and **6** (V *vs.* Ag/AgCl)[a]

Compound	$E_{ox}^{\ddagger}$/V	$E_{1red}^{\ddagger}$/V	$E_{2red}^{\ddagger}$/V	$E_{3red}^{\ddagger}$/V	ΔE_{1-2}/V	K_{dispr}[b]/ dm^3 mol^{-1}	E_A/eV
2a	+1.23	−0.89		—	—	—	1.65
2b	+1.33	−0.82		—	—	—	1.72
2c	+1.33	−0.79		—	—	—	1.75
2d	+1.34	−0.77		—	—	—	1.77
2e	+1.36	−0.70	−0.77	—	0.07	6.5×10^{-2}	1.85
2f	+1.37	−0.67	−0.75	−1.32	0.08	4.4×10^{-2}	1.88
2g	+1.47	−0.53	−0.62	−1.34	0.09	3.0×10^{-2}	2.03
2h	+1.42	−0.59	−0.68	−1.37	0.09	3.0×10^{-2}	1.96
2i	+1.55	−0.40	−0.50	−1.31	0.10	2.0×10^{-2}	2.17
				−1.56[c]			
2j	+1.40	−0.63	−0.75	−1.34	0.12	9.2×10^{-3}	1.92
2k	+1.51	−0.58	−0.71	−1.33	0.13	6.3×10^{-3}	1.98
2l	+1.49	−0.52	−0.66	−1.38	0.14	4.2×10^{-3}	2.04
3a	+0.71	−1.16		—	—	—	1.36
3c	+0.77	−1.04	−1.14	—	0.10	2.0×10^{-2}	1.49
3d	+0.77	−1.03	−1.13	—	0.10	2.0×10^{-2}	1.50
3e	+0.87	−0.97	−1.06	—	0.09	3.0×10^{-2}	1.56
3f	+0.89	−0.93	−1.03	−1.44	0.10	2.0×10^{-2}	1.60
3g	+1.00	−0.84	−0.96	−1.50	0.12	9.2×10^{-3}	1.70
3i	+1.11	−0.70	−0.86	−1.50	0.16	1.9×10^{-3}	1.85
3j	+0.84	−0.93	−1.05	−1.42	0.12	9.2×10^{-3}	1.60
3k	+0.91	−0.91	−1.02	−1.50	0.11	1.4×10^{-2}	1.63
3m	+0.90	−0.94	−1.06	−1.43	0.12	9.2×10^{-3}	1.59
5	+1.41	−0.56	−0.79	−1.39	0.23	1.3×10^{-4}	2.00
6	+1.46	−0.12	−0.68	−1.21	0.56	3.2×10^{-10}	2.46

[a] Solvent acetonitrile; electrolyte 0.2 M $Et_4N^+BF_4^-$; scan rate 100 mV s^{-1}. All potentials given in the table were measured *vs.* Fc^0/Fc^+ couple as internal reference and recalculated to the Ag/AgCl scale. (The Fc^0/Fc^+ couple was observed at +0.45 V *vs.* Ag/AgCl under these conditions.) [b] Calculated using equation $\Delta E_{1-2} = E_{1red}^{\ddagger} - E_{2red}^{\ddagger} = -0.059 \log K_{dispr}$. [c] A fourth quasireversible reduction wave, $E_{4red}^{\ddagger}$, was observed for **2i**.

Table 7 Correlations of the electrochemical reduction/oxidation waves for compounds **2** and **3** according to eqn. (3)

Entry	Compound	CV wave	$E_0^{\ddagger}$/V	$\rho^-/10^{-2}$ V	r^a	n^b
1	**2**	$E_{ox}^{\ddagger}$	0.935 ± 0.015	12.0 ± 0.7	0.9908	7[c]
2	**2**	$E_{1red}^{\ddagger}$	−1.396 ± 0.011	19.5 ± 0.5	0.9981	7[c]
3	**2**	$E_{1red}^{\ddagger}$	−1.420 ± 0.012	20.0 ± 1.0	0.9974	4[d]
4	**2**	$E_{2red}^{\ddagger}$	−1.427 ± 0.015	18.2 ± 1.2	0.9954	4[d]
5	**3**	$E_{ox}^{\ddagger}$	0.267 ± 0.021	16.5 ± 1.0	0.9910	7[c]
6	**3**	$E_{1red}^{\ddagger}$	−1.598 ± 0.011	17.5 ± 0.5	0.9976	7[c]
7	**3**	$E_{1red}^{\ddagger}$	−1.585 ± 0.012	17.2 ± 0.7	0.9967	6[e]
8	**3**	$E_{2red}^{\ddagger}$	−1.577 ± 0.013	14.1 ± 0.8	0.9941	6[e]

[a] Correlation coefficient. [b] Number of points. [c] Points for **2a**,**c**–**g**,**i** (or **3a**,**c**–**g**,**i**) were used in the correlation. [d] Points for **2e**–**g**,**i** were used in the correlation. [e] Points for **2c**–**g**,**i** were used in the correlation.

(Table 6). The thermodynamic stability of radical anions from compounds **5** and **6** is greater than that for **2** or **3**, and the value $K_{dispr} = 3.2 \times 10^{-10}$ dm^3 mol^{-1} for **6** is even comparable with that for strong fluorene acceptors and for TCNQ derivatives (10^{-8}–10^{-12} dm^3 mol^{-1}).

Electronic absorption spectra in the ICT region

Intramolecular donor–acceptor interaction in compounds **2** and **3** was also manifested in their electron absorption spectra: in the visible region additional absorption bands corresponding to ICT transitions appeared. The intramolecular nature of this transition was corroborated by studies of concentration dependencies of the CT band intensities.

The maxima of the ICT bands for the compounds **2** and **3** in various solvents are summarized in Table 8. For both series of compounds a bathochromic shift of λ_{ICT} with increasing solvent polarity was observed, which is indicative of increased polarity of the excited state in compounds **2** and **3** as compared to the ground state.

The transition from compounds **2** to compounds **3** is accompanied by a bathochromic shift of the ICT band (for **2** λ_{ICT} = 440–550 nm, for **3** λ_{ICT} = 530–620 nm) and a decrease in its intensity (Fig. 9, Table 1). This is in contrast with TCNQ and TCNE where substitution of the second cyano group is accompanied by a hypsochromic shift of the ICT band.[5] A bathochromic shift of the ICT band was also observed when the number of electron-withdrawing substituents in compounds **2** and **3** increased.

A quantitative estimation of the effect of substituents in the fluorene ring of compounds **2** and **3** upon the energies of ICT bands was performed using eqn. (5), where $h\nu_{ICT}$ is the ICT

$$h\nu_{ICT} = h\nu^0_{ICT} + \rho^-\Sigma\sigma_p^- \quad (5)$$

energy defined by the maxima of the ICT band (λ_{ICT}), $h\nu^0_{ICT}$ is $h\nu_{ICT}$ for the reference compound (unsubstituted benzene rings in fluorenes, $\Sigma\sigma_p^- = 0$), ρ^- is a parameter showing ICT energy sensitivity to substituents, and $\Sigma\sigma_p^-$ is the same as in eqn. (3).

The data for the influence of substituents in various solvents are given in Table 9 and they show good correlation in all the cases [$r = -(0.990 - 0.999)$ for **2** and $r = -(0.955 - 0.999)$

Table 8 Maxima of ICT bands (λ_{ICT}, nm) for compounds **2**, **3** and **9** with dimethylamino grouped as donor moiety in various solvents, 25 °C

Entry					Solvent										
					Dioxane	Benzene	Chlorobenzene	Acetic acid	*o*-Dichlorobenzene	Acetone	DMF	AN	DMSO	Formic acid	Formamide
1	$\varepsilon^{a,b}$				2.209	2.284	5.62	6.15	9.93	20.74	36.7	37.5	48.9	57.9	111.5
2	$n_D^{20\,b,c}$				1.4233	1.5011	1.5218	1.3716	1.5515[g]	1.3588	1.4272	1.3416	1.4783	1.3714	1.4475
3	$(\varepsilon - 1)/(2\varepsilon + 1)$				0.2231	0.2306	0.3775	0.3872	0.4281	0.4647	0.4798	0.4803	0.4848	0.4872	0.4933
4	$(n^2 - 1)/(n^2 + 2)$				0.2548	0.2947	0.3049	0.2271	0.3193	0.2200	0.2569	0.2105	0.2832	0.2270	0.2675
5	$B^{b,d}/cm^{-1}$				237	48	38	139	(38)[h]	224	291	160	362	131	270
6	$E^{b,e}$/kcal				4.2	2.1	0	14.6	(0)	2.1	2.6	5.2	3.2	16.7	14.5
					λ_{ICT}/nm										
Entry	Compound	X	Y	$\Sigma\sigma_p^{-}$[f]											
7	**2a**	H	H	2.54	441.4	443.0	441.5	444.0	443.8	443.8	453.2	445.6	457.7	—	—
8	**2b**	H	$CON(CH_3)_2$	—	454.0	454.7	454.9	455.7	455.6	461.9	471.7	464.1	478.2	469.7	472.8
9	**2c**	H	$COOCH_3$	3.176	460.0	460.6	459.3	459.3	460.2	469.4	482.6	470.7	486.1	471.5	476.8
10	**2d**	H	$COOC_4H_9$	3.214	458.6	460.2	459.7	459.7	458.9	469.7	479.2	471.1	487.1	470.6	477.3
11	**2e**	H	CN	3.54	464.6	464.0	465.7	467.9	467.9	476.8	489.6	479.2	495.8	477.8	483.3
12	**2f**	H	NO_2	3.81	472.8	472.3	475.8	475.3	476.8	486.6	497.4	488.3	513.1	487.5	495.8
13	**2g**	NO_2	$COOCH_3$	4.446	492.2	489.0	492.3	495.8	493.8	512.8	525.7	513.8	533.3	511.5	519.5
15	**2h**	NO_2	$CON(C_{10}H_{21})_2$	—	485.9	484.7	488.0	494.3	489.0	503.2	515.4	505.0	524.4	513.1	*i*
15	**2i**	NO_2	NO_2	5.08	505.5	504.8	513.3	512.3	513.1	528.0	543.3	531.2	552.2	528.8	536.7
16	**3a**	H	H	2.54	528.0	526.9	531.4	533.6	534.2	542.2	556.2	547.0	563.7	*j*	570.8
17	**3b**	H	$CON(CH_3)_2$	—	531.9	529.7	533.0	536.3	537.1	545.8	558.0	550.7	565.6	*j*	569.5
18	**3c**	H	$COOCH_3$	3.176	542.9	540.0	547.0	548.8	547.6	558.6	570.1	561.8	577.4	*j*	579.4
19	**3d**	H	$COOC_4H_9$	3.214	542.3	540.0	544.7	548.2	547.6	557.4	568.8	560.2	577.4	*j*	580.0
20	**3e**	H	CN	3.54	539.4	533.6	539.7	546.4	543.5	556.1	567.5	559.5	574.7	*j*	578.0
21	**3f**	H	NO_2	3.81	551.9	547.4	552.2	561.2	561.2	570.7	582.8	575.7	590.3	*j*	598.1
22	**3g**	NO_2	$COOCH_3$	4.446	564.3	559.3	568.2	578.0	571.4	588.2	600.2	591.3	605.3	606.8	610.5
23	**3i**	NO_2	NO_2	5.08	570.8	562.4	574.1	583.4	586.7	598.1	609.0	602.4	615.8	614.3	620.3
24	**10a**	H	NO_2	3.81	513.3	512.8	516.5	519.8	519.8	532.5	544.7	532.8	552.8	*j*	545.3
25	**10b**	NO_2	NO_2	5.08	541.1	539.1	552.5	552.5	556.2	568.2	582.8	570.1	590.3	578.7	584.3

[a] Relative permittivity. [b] From ref. 36. [c] Refraction index. [d] Basicity of the solvent. [e] Electrophilicity of the solvent. [f] σ_p^{-} = 0 (H), 0.636 (COOMe), 0.674 (COOBu), 1.00 (CN), 1.270 (NO_2); see ref. 37. [g] From ref. 38. [h] Accepted to be equal to that for chlorobenzene. [i] The compound is insoluble in this solvent. [j] Compounds reacted with formic acid giving salts; no ICT bands were observed.

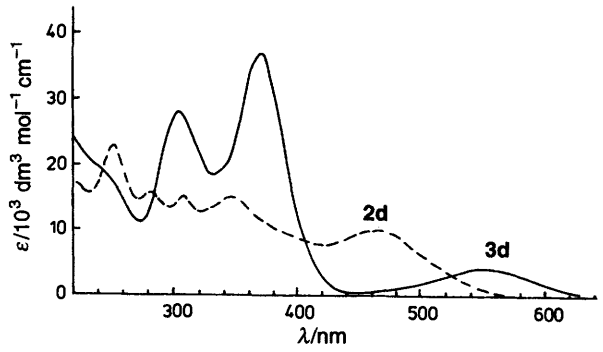

Fig. 9 Electronic absorption spectra of compounds **2d** and **3d** in acetonitrile, 25 °C

for **3**].** The sensitivity of ICT energies to the influence of substituents, ρ^-, decreases when passing from compounds **2** to compounds **3** (approximately by a factor of 2). This is somewhat unexpected as ρ_{1red}^- values for the electrochemical experiments (for the reaction A ⟶ A$^{\cdot -}$) are very similar for compounds **2** and **3**, and for compound **2**, ρ^- values from CV data (0.195 ± 0.005 V, Table 7) and from spectral data (0.175 ± 0.008 eV, Table 9) approximately coincide. Recently we have investigated intramolecular charge transfer in sulfur-containing fluorene acceptors of type **9**;[39] ρ^- values of −0.121 ± 0.012 eV found for **9** in DMF lie between those for compounds **2** and **3**.

For both series of compounds, *i.e.* **2** and **3**, a tendency of ρ^- to increase with increasing solvent polarity was observed. However, there are also some dissimilarities in the nature of the variations of the sensitivity ρ^- parameters with changes in the medium polarity for compounds **2** and **3**. Thus, the plot of ρ^- *vs.* $\varepsilon^{0.5}$ displayed a curvilinear dependence (increasing ρ^- with increase of $\varepsilon^{0.5}$) for **2**, whereas a bell-like dependence with ρ_{max}^- at $\varepsilon \approx 25$ for **3** was observed (Fig. 10).

In a previous paper,[40] a satisfactory correlation (r 0.97) of the ICT energy in 2,4,5,7-tetranitro-9-dimethylaminomethylenefluorene (**10b**) of the function $\varepsilon^{0.5}$ was achieved; this function gave a better correlation than the Kirkwood polarity function $[(\varepsilon - 1)/(2\varepsilon + 1)]$.[41] In our case a single parameter, *i.e.* the medium polarity [the functions $\varepsilon^{0.5}$ or $(\varepsilon - 1)/(2\varepsilon + 1)$] were insufficient to describe the solvent effects upon ICT energies, since most of the solvents used have pronounced electrophilic or basic properties which cannot be neglected.

For a quantitative estimation of the solvent influence upon ICT energies we used the Koppel–Palm four-parameters equation[36] which separately considers polarity $[(\varepsilon - 1)/(2\varepsilon + 1)]$, polarizability $[(n^2 - 1)/(n^2 + 2)]$, basicity (B) and electrophilicity (E) of the solvent [eqn. (6)]; here y, p, b and e

$$h\nu_{ICT} = h\nu_{ICT}^g + y\frac{\varepsilon - 1}{2\varepsilon + 1} + p\frac{n^2 - 1}{n^2 + 2} + bB + eE \quad (6)$$

are sensitivity parameters to the above mentioned effects of the solvent, respectively. Correlations of ICT energies using eqn. (6) showed that in all cases it is only polarity and basicity of the solvent that prove to be statistically relevant.†† By way of an example, a form of eqn. (6), can be given for compound **3i** [eqn. (7)].

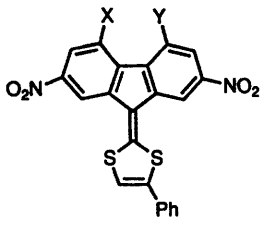

9

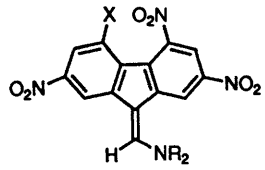

10 a X = H, R = Me
10 b X = NO_2, R = Me

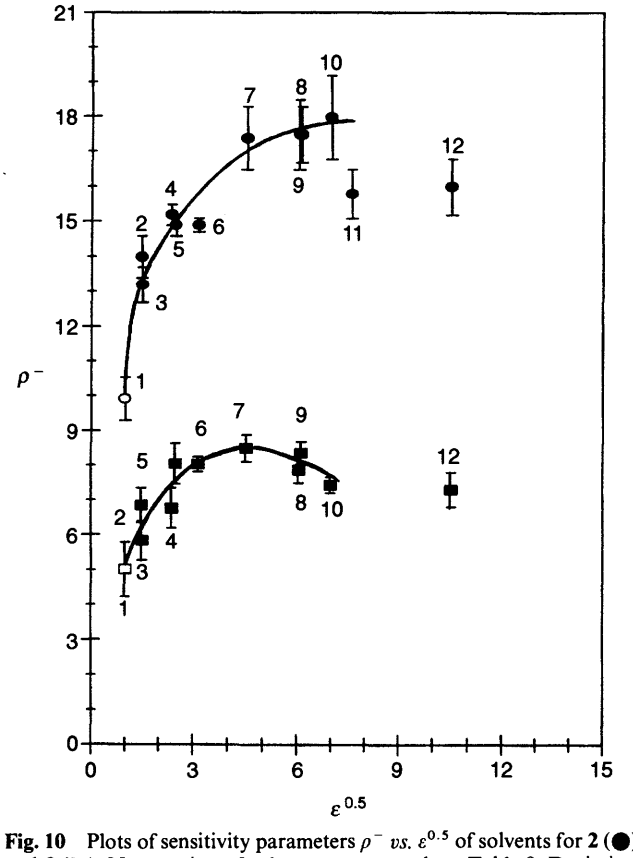

Fig. 10 Plots of sensitivity parameters ρ^- *vs.* $\varepsilon^{0.5}$ of solvents for **2** (●) and **3** (■). Numeration of solvents corresponds to Table 9. Deviation of points for formic acid (11) and formamide (12) are discussed in the text; ○ and □ are calculated values for the gas phase.

$$h\nu_{ICT}[eV] = (2.41 \pm 0.02) - (0.52 \pm 0.06)\frac{\varepsilon - 1}{2\varepsilon + 1} - (0.18 \pm 0.19)\frac{n^2 - 1}{n^2 + 2} - (23.1 \pm 5.7) \times 10^{-5}B + (25.6 \pm 10.8) \times 10^{-4}E \quad (7)$$

$$n = 11, \quad s = 0.0011, \quad r = 0.981$$

Treatment of the data of Table 8 using eqn. (8) yielded

$$h\nu_{ICT} = h\nu_{ICT}^g + y\frac{\varepsilon - 1}{2\varepsilon + 1} + bB \quad (8)$$

satisfactory correlation parameters (Table 10). We have analysed the changes in the ICT energies in compounds **2** and **3** in the gas phase calculated by eqn. (8) ($h\nu_{ICT}^g$, Table 10). Here, as in the case of similar dependences in various solvents, good linear dependences on $\Sigma\sigma_p^-$ constants according to eqn. (5)

** Both scales of substituents, *i.e.* Hammett's constants σ_p and nucleophilic constants σ_p^-, give close correlation coefficients r. So, from this viewpoint, it is impossible to choose between these two scales of substituents as they have been correlated between each other for the substituents used (correlation coefficient between σ_p and σ_p^- for the substituents used is 0.994). However, we believe that the scale of σ_p^- is more applicable due to the possibility of polar resonance (as a result of ICT) displayed by structures **7** and **8**.

†† The use of a five-parameter equation including the density of the energy of cohesion (δ^2) proposed by Makitra and Pirig[42] indicated that the parameter δ^2 is also statistically irrelevant in this case.

Table 9 Correlations of the ICT energies for compounds **2** and **3** according to eqn. (5)

Entry	Solvent	ε	$\varepsilon^{0.5}$	$h\nu^{\circ}_{ICT}$/eV	$\rho^{-} \times 10^2$/eV	r^a	n^b
				2a,c–g,i			
1	Gas phase[c]	1	1	3.126 ± 0.013	−9.93 ± 0.61	−0.9932	7
2	Dioxane	2.209	1.486	3.157 ± 0.012	−14.0 ± 0.6	−0.9961	7
3	Benzene	2.284	1.511	3.127 ± 0.010	−13.2 ± 0.5	−0.9965	7
4	Chlorobenzene	5.62	2.370	3.191 ± 0.007	−15.2 ± 0.3	−0.9987	7
5	Acetic acid	6.15	2.480	3.174 ± 0.006	−14.9 ± 0.3	−0.9992	7
6	*o*-Dichlorobenzene	9.93	3.151	3.174 ± 0.005	−14.9 ± 0.2	−0.9993	7
7	Acetone	20.74	4.554	3.212 ± 0.020	−17.4 ± 0.9	−0.9929	7
8	Dimethylformamide	36.7	6.058	3.155 ± 0.020	−17.5 ± 1.0	−0.9920	7
9	Acetonitrile	37.5	6.124	3.204 ± 0.016	−17.5 ± 0.8	−0.9950	7
10	Dimethyl sulfoxide	48.9	6.993	3.135 ± 0.025	−18.0 ± 1.2	−0.9895	7
11	Formic acid	57.9	7.609	3.141 ± 0.012	−15.8 ± 0.7	−0.9962	6[d]
12	Formamide	111.5	10.56	3.113 ± 0.013	−16.0 ± 0.8	−0.9952	6[d]
				3a,c–g,i			
1	Gas phase[c]	1	1	2.585 ± 0.025	−5.18 ± 1.18	−0.8910	7
				2.572 ± 0.016	−5.02 ± 0.78	−0.9545	6[e]
2	Dioxane	2.209	1.486	2.519 ± 0.016	−6.96 ± 0.76	−0.9718	7
				2.510 ± 0.010	−6.86 ± 0.49	−0.9900	6[e]
3	Benzene	2.284	1.511	2.501 ± 0.020	−5.99 ± 0.96	−0.9409	7
				2.489 ± 0.012	−5.85 ± 0.56	−0.9820	6[e]
4	Chlorobenzene	5.62	2.370	2.507 ± 0.020	−6.92 ± 0.97	−0.9540	7
				2.496 ± 0.012	−6.78 ± 0.57	−0.9861	6[e]
5	Acetic acid	6.15	2.480	2.529 ± 0.018	−8.18 ± 0.86	−0.9733	7
				2.520 ± 0.012	−8.06 ± 0.59	−0.9896	6[e]
6	*o*-Dichlorobenzene	9.93	3.151	2.534 ± 0.019	−8.18 ± 0.89	−0.9716	7
				2.522 ± 0.005	−8.04 ± 0.22	−0.9985	6[e]
7	Acetone	20.74	4.554	2.506 ± 0.016	−8.63 ± 0.77	−0.9809	7
				2.497 ± 0.008	−8.51 ± 0.39	−0.9957	6[e]
8	Dimethylformamide	36.7	6.058	2.438 ± 0.016	−8.00 ± 0.08	−0.9769	7
				2.428 ± 0.008	−7.88 ± 0.38	−0.9955	6[e]
9	Acetonitrile	37.5	6.124	2.487 ± 0.016	−8.51 ± 0.76	−0.9805	7
				2.477 ± 0.007	−8.38 ± 0.32	−0.9971	6[e]
10	Dimethyl sulfoxide	48.9	6.993	2.395 ± 0.015	−7.55 ± 0.72	−0.9776	7
				2.386 ± 0.005	−7.44 ± 0.23	−0.9981	6[e]
12	Formamide	111.5	10.56	2.375 ± 0.019	−7.45 ± 0.92	−0.9641	7
				2.364 ± 0.010	−7.31 ± 0.50	−0.9907	6[e]

[a] Correlation coefficient. [b] Number of points. [c] Values of $h\nu^{g}_{ICT}$ calculated from the data of Table 8 using eqn. (8) were used (see Table 10). [d] Without point for **2a**. [e] Deleted most deviated point for **3e** (deviations from the straight line are 0.027–0.037 eV).

were observed, and the parameter ρ^{-} for compounds **2** is twice as high as that for compounds **3** (Table 9). Estimation of the isoparametric point at which the ICT energies in compounds of series **2** will coincide with those for analogous compounds of series **3** gave the value $\Sigma\sigma_p^{-} = 11.3$ (in the gas phase), *i.e.* about 9 nitro groups which is hardly experimentally attainable.

Analysis of the influence of the structure of compounds **2** and **3** on the parameters y and b showed that for both series of compounds (*i.e.* **2** and **3**) the parameters b were closely allied and do not vary, within experimental error, when the substituents X and Y change. For compounds **2i** and **3i** the ICT energy sensitivities to the solvent polarity are closely related; when the number of electron withdrawing substituents in compounds **2** and **3** decreases, the parameter of sensitivity y drops for both series of compounds, with a more dramatic decrease in y being observed for compounds **2**, and the parameters of y differ by 3 times for compounds **2a** and **3a** (Fig. 11, Table 10).

Table 8 compares the measured maxima of the ICT bands for compounds **10a,b** and Table 10 demonstrates the parameters of the correlation eqn. (8) for the given compounds. The above tables indicate that the donor capacity of the methylene fragment increases in the expected range: *i.e.* based on their ICT energies, compounds **10** are between **2** and **3** (variations in the ICT energies in the transition **2** ⟶ **10** ⟶ **3** are 0.15 ± 0.05 eV).

A much lower value for the ICT energy (*i.e.* a longer wavelength band for ICT) is observed in compound **6**: λ_{ICT} = 646 nm, $h\nu_{ICT}$ = 1.92 eV (acetonitrile), [*cf.* compounds **2i**: λ_{ICT} = 531.2 nm, $h\nu_{ICT}$ = 2.33 eV and **3i**: λ_{ICT} = 602.4 nm, $h\nu_{ICT}$ = 2.06 eV (Table 8)] indicating a more effective intramolecular donor–acceptor interaction in compound **6**.

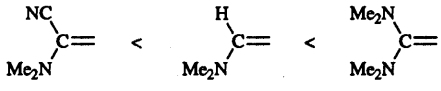

Decoloration of compounds **2** and **3** was observed upon their dissolution in sulfuric acid (and in formic acid for **3a–f**) as a result of salt formation; subsequent dilution with water quantitatively regenerated compounds **2** and **3**. Decoloration of compounds **2** was not observed in formic acid, but deviation of the point for **2** in formic acid on Fig. 10 can be explained by this acid–base interaction.

Spectroelectrochemical studies

CV measurements (discussed above) showed that reduction of compounds **2** and **3** leads to the formation of radical anion and dianion species and oxidation leads to the radical cation. Undoubtedly, the negative charge in $A^{\bullet -}$ and A^{2-} is delocalized on the fluorene ring, whereas the positive charge in $A^{\bullet +}$ is localized on the amino group. Spectral investigation confirmed an important ICT in the compounds **2** and **3** (structures **7** and **8**).

Transitions A ⟶ $A^{\bullet -}$ ⟶ A^{2-} or A ⟶ $A^{\bullet +}$ should lead to spectroscopic changes: in the $A^{\bullet -}$ and A^{2-} states the fluorene

Table 10 Correlations of the ICT energies in compounds **2** and **3** according to eqn. (8)

Entry	Compound	X	Y	$\Sigma\sigma_p^-$	$h\nu^g_{ICT}$/eV	y	$b \times 10^5$	R^a	n
1	**2a**	H	H	2.54	2.860 ± 0.022	−0.121 ± 0.082	−18.3 ± 7.3	0.8305	9[b]
2	**2b**	H	$CONMe_2$	(3.05)[c]	2.835 ± 0.024	−0.273 ± 0.083	−25.1 ± 7.5	0.9035	11
3	**2c**	H	COOMe	3.176	2.804 ± 0.025	−0.246 ± 0.086	−32.0 ± 7.8	0.9130	11
4	**2d**	H	COOBu	3.214	2.810 ± 0.026	−0.258 ± 0.083	−31.4 ± 7.6	0.9185	11
5	**2e**	H	CN	3.54	2.792 ± 0.022	−0.311 ± 0.074	−31.7 ± 6.8	0.9424	11
6	**2f**	H	NO_2	3.81	2.757 ± 0.028	−0.336 ± 0.095	−36.1 ± 8.7	0.9256	11
7	**2g**	NO_2	COOMe	4.446	2.686 ± 0.022	−0.407 ± 0.075	−40.4 ± 6.8	0.9639	11
8	**2h**	NO_2	$CON(C_{10}H_{21})_2$	—	2.706 ± 0.027	−0.424 ± 0.093	−32.3 ± 8.5	0.9394	10[d]
9	**2i**	NO_2	NO_2	5.08	2.609 ± 0.024	−0.447 ± 0.081	−33.1 ± 7.4	0.9546	11
10	**3a**	H	H	2.54	2.480 ± 0.029	−0.358 ± 0.106	−28.7 ± 9.5	0.9152	10[e]
11					2.462 ± 0.020	−0.310 ± 0.074	−25.4 ± 6.5	0.9481	9[b]
12	**3b**	H	$CONMe_2$	(3.05)[c]	2.459 ± 0.024	−0.333 ± 0.088	−28.0 ± 7.8	0.9343	10[e]
13					2.444 ± 0.018	−0.296 ± 0.066	−25.5 ± 5.9	0.9556	9[b]
14	**3c**	H	COOMe	3.176	2.407 ± 0.020	−0.330 ± 0.072	−26.2 ± 6.4	0.9509	10[e]
15					2.396 ± 0.015	−0.301 ± 0.056	−24.1 ± 5.0	0.9663	9[b]
16	**3d**	H	COOBu	3.214	2.409 ± 0.022	−0.324 ± 0.079	−27.2 ± 7.1	0.9425	10[e]
17					2.396 ± 0.016	−0.290 ± 0.059	−24.9 ± 5.2	0.9628	9[b]
18	**3e**	H	CN	3.54	2.442 ± 0.019	−0.361 ± 0.069	−30.4 ± 6.2	0.9636	10[e]
19					2.429 ± 0.012	−0.329 ± 0.046	−28.2 ± 4.0	0.9821	9[b]
20	**3f**	H	NO_2	3.81	2.394 ± 0.024	−0.402 ± 0.086	−28.2 ± 7.7	0.9478	10[e]
21					2.378 ± 0.014	−0.361 ± 0.053	−25.3 ± 4.7	0.9762	9[b]
22	**3g**	NO_2	COOMe	4.446	2.358 ± 0.026	−0.482 ± 0.088	−23.5 ± 8.1	0.9386	11
23					2.345 ± 0.018	−0.415 ± 0.064	−28.2 ± 5.7	0.9709	10[e]
24					2.334 ± 0.011	−0.386 ± 0.043	−26.2 ± 3.8	0.9856	9[b]
25	**3i**	NO_2	NO_2	5.08	2.354 ± 0.022	−0.548 ± 0.074	−22.2 ± 6.7	0.9622	11
26					2.343 ± 0.016	−0.496 ± 0.058	−25.8 ± 5.2	0.9797	10[e]
27					2.333 ± 0.011	−0.470 ± 0.039	−24.0 ± 3.5	0.9900	9[b]
28	**10a**	H	NO_2	3.81	2.546 ± 0.021	−0.356 ± 0.077	−30.6 ± 6.8	0.9580	9[b]
29	**10b**	NO_2	NO_2	5.08	2.445 ± 0.018	−0.484 ± 0.068	−25.4 ± 6.0	0.9730	9[b]

[a] Multiply correlation coefficient. [b] Without points for formic acid and formamide. [c] The mean value, calculated on the basis of correlation eqn. (5) for compounds **2a**, **c–g**, **i** in various solvents (Table 9) and values of $h\nu_{ICT}$ for **2b** in the same solvents (Table 8). From this value of $\Sigma\sigma_p^-$ we have calculated σ_p^- for $CONMe_2$ = 0.51. [d] Without point for formamide (the compound is insoluble in this solvent). [e] Without point for formic acid.

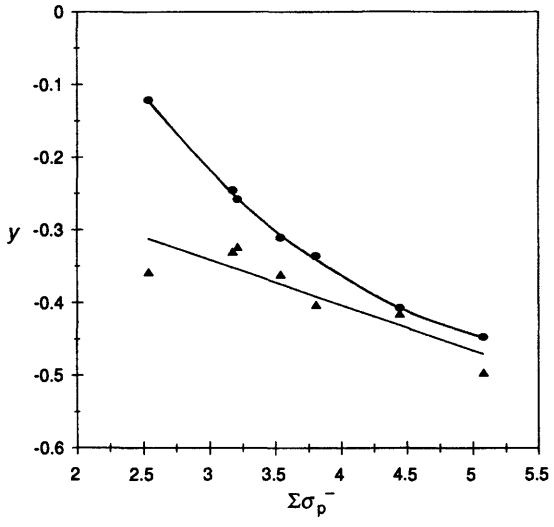

Fig. 11 Plots of sensitivity parameters to solvent polarity y *vs.* $\Sigma\sigma_p^-$ for compounds **2** (●) and **3** (▲)

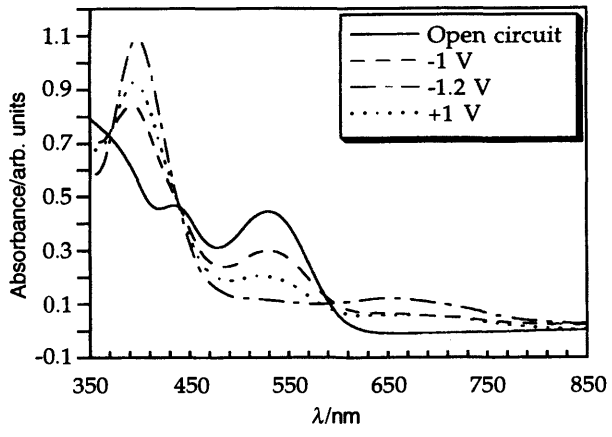

Fig. 12 Absorption spectra in the visible region for compound **2i** at various applied potentials, in acetonitrile, electrolyte $Bu_4N^+BF_4^-$ (0.2 M)

ring does not exhibit electron accepting properties and in the $A^{\bullet+}$ state the amino group does not exhibit donating properties. One should expect that this will result in the disappearance of the ICT bands in the electron absorption spectra. To confirm this we carried out spectroelectrochemical experiments using compound **2i** (Fig. 12). Actually, in both cases (*i.e.* when positive or negative potential is applied) the intensity of the ICT band (531.2 nm, Table 1) decreased and, at the appropriate voltage, disappeared.‡‡ Both processes, reduction and oxidation, lead to the appearance of a new intensive absorbance at 400 nm which is absent in the neutral compound **2i**. In addition, for the reduction process an absorbance in the 650 nm region appeared which can be assigned to a long-wave absorbance of the radical anion (or dianion).

‡‡ Some disagreement in potentials with CV data are explained by the considerable potential drop due to uncompensated solution resistance in the thin layer cell.

Sensitization of poly-*N*-(2,3-epoxypropyl)carbazole (PEPC) photoconductivity

Earlier, we have shown[43] that butyl 2,7-dinitro-9-dicyanomethylenefluorene-4-carboxylate (**1d**) sensitizes the photoconductivity of carbazole-containing polymers, and as a sensitizer of photothermoplastic materials it excels 2,4,7-trinitro-9-dicyanomethylenefluorene (**1f**), which is widely used for these purposes. Substitution of the electron-withdrawing cyano group by the donating dimethylamino-substituent will decrease the electron accepting properties of the molecule.

From this point of view one should have expected a decrease in the ability of compounds **2** and **3** (compared to **1**) to form intermolecular charge transfer complexes (CTC) with electron donors and, hence, decreased sensitization of photoconductivity of polymer donors of the PEPC type. On the other hand, the latest investigations[44] demonstrate the potential to improve the sensitizing ability of the acceptors with ICT in the region of their intrinsic absorption.

We have, therefore, made a comparative study of the effect of the addition of compounds **1d**, **2d** and **3d** on the spectral distribution of electrophotographic sensitivity ($S_{\Delta V}$, $m^2\ J^{-1}$) of thin (*i.e.* 1.2–1.4 μm) PEPC films. As expected, a hypsochromic shift of the red-wave border of photosensitivity, and a decrease in the value for $S_{\Delta V}$ in the long-wave region, are both observed in the order **1d** ⟶ **2d** ⟶ **3d** (Fig. 13) in agreement with an increase in the electron-accepting properties of the molecules (**1d** > **2d** > **3d**). Concomitantly, in the short-wave region, increased photosensitivity of the films using compound **2d** is observed, which in the ICT region of **2d** (460–480 nm, Table 8) even exceeds that for **1d**. This can be accounted for by the fact that the acceptor **2d** sensitizes PEPC photoconductivity by two mechanisms: *i.e.* by the donor–acceptor interaction at the expense of formation of intermolecular CTC with the PEPC carbazole nuclei, and by the spectral sensitization similar to that realized on dyes. No similar increase in photoconductivity was observed in the case of compound **3d**, which is apparently due to its weaker acceptor ability (E_A = 1.77 eV for **2d** and 1.50 eV for **3d**, Table 6) and low molar extinction coefficient (about half that of compounds **2**, Fig. 9, Table 1).

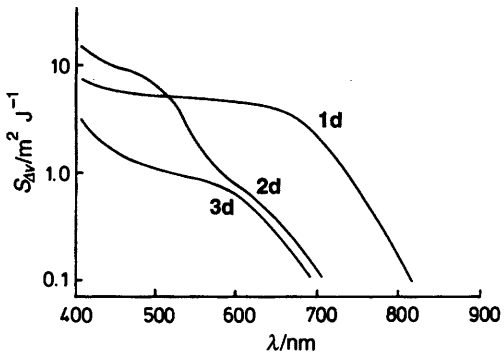

Fig. 13 Spectral distribution of electrophotographic sensitivity ($S_{\Delta V}/m^2\ J^{-1}$) of PEPC films sensitized by fluorene derivatives **1d**, **2d** and **3d**

Experimental

General

Mps were recorded on a Kofler hot-stage microscope apparatus and are uncorrected. UV–VIS spectra were recorded on a Specord M-40 spectrophotometer, with solvents as indicated. IR spectra were recorded on a Carl Zeiss UR-20 spectrometer in Nujol. ^1H MMR spectra were recorded on a Varian GEMINI-200 instrument, operating at 200 MHz. Chemical shifts, given in ppm, are relative to tetramethylsilane (Me_4Si) as internal standard. All *J* values are in Hz. TLC analyses were performed using Chemapol 'Silufol UV 254' pre-coated silica aluminium backed sheets; eluents were benzene–dioxane, (4–8):1 v/v or toluene–dioxane–heptane, (4–8):(1–3):1 v/v mixtures. For column chromatography, Chemapol silica gel (100–160 mesh or 40–100 mesh) was employed, with benzene or benzene–acetone, (2–5):1 v/v as eluents. Dioxane, benzene, acetic acid, acetone, dimethylformamide, acetonitrile, dimethyl sulfoxide, formic acid and formamide for UV–VIS spectral measurements were purified as described earlier.[45] Chlorobenzene and *o*-dichlorobenzene were stirred with sulfuric acid, washed with water, dried over $CaCl_2$ and twice distilled from P_4O_{10}.

Compounds **1a**,[46] **1c**,[47] **1d**,[43] **1e**,[48] **1f**,[46] **1g**[49] and **1i**,[46] were obtained as described earlier.

N,N-Dimethyl-2,7-dinitro-9-dicyanomethylenefluorene-4-carboxyamide 1b

2,7-Dinitro-9-oxofluorene-4-carboxylic acid[50] (20.0 g, 64 mmol), thionyl chloride (8.0 cm^3, 110 mmol) and DMF (4 drops) in dry chloroform (70 cm^3) were refluxed for 2 h. The reaction mixture was cooled to room temperature and poured into 33% aqueous dimethylamine (200 cm^3). The solid was filtered, washed with water and dried, yielding *N,N*-dimethyl-2,7-dinitro-9-oxofluorene-4-carboxamide (18.2 g, 84%), mp 272–274 °C (from acetic acid).

This compound (10.0 g, 29 mmol) and malononitrile (5.8 g, 88 mmol) were stirred in DMF (100 cm^3) at 60–70 °C for 2 h. After cooling, the bright yellow solid which precipitated, was washed with methanol and dried, yielding compound **1b** (8.0 g, 80%), mp 272–273 °C. Recrystallization by dissolving in DMF (110 cm^3) and subsequent dilution with methanol (250 cm^3) did not change the melting point (Found: C, 58.7; H, 2.8; N, 17.9. $C_{19}H_{11}N_5O_5$ requires C, 58.6; H, 2.85; N, 18.0%).

N,N-Didecyl-2,5,7-trinitro-9-dicyanomethylenefluorene-4-carboxyamide 1h

2,5,7-Trinitro-9-oxofluorene-4-carboxylic acid[50] (30.0 g, 83 mmol), thionyl chloride (100 cm^3) and DMF (4 drops) were refluxed for 1 h. Excess thionyl chloride was removed under reduced pressure and the residue was dissolved in dry dioxane (250 cm^3). Didecylamine (24.8 g, 83 mmol) and triethylamine (11.7 cm^3, 84 mmol) were added to this solution, the mixture was stirred for 1.5 h at room temperature and poured into water (800 cm^3). The resulting brown oil crystallized after some time, the solid was collected and washed with water yielding a crude light-brown product (52.5 g, 98.5%), mp 65–70 °C. Purification by column chromatography (3 × 20 cm) on silica gel (100–400 mesh) with benzene as eluent, followed by recrystallization from propan-2-ol gave *N,N*-didecyl-2,5,7-trinitro-9-oxofluorene-4-carboxyamide (37.2 g, 70%) as light-yellow crystals, mp 70.5–72.0 °C (Found: C, 63.8; H, 7.25; N, 8.8. $C_{34}H_{46}N_4O_8$ requires C, 63.95; H, 7.25; N, 8.75%); ν/cm^{-1} 3120, 3110 (C–H), 1740 (C=O, fluorenone), 1650 (C=O, amide), 1545 (NO_2) and 1355 (NO_2).

The above amide (30.0 g, 47 mmol) and malononitrile (8.0 g, 121 mmol) were stirred in DMF (50 cm^3) at room temperature for 1.5 h. The solution was diluted with propan-2-ol (500 cm^3), after 5 h a solid was filtered and washed with propan-2-ol, yielding amide **1h** (31.4 g, 97.5%), mp 135–136 °C (from dioxane–propan-2-ol, 1:5 v/v) (Found: C, 64.8; H, 6.65; N, 12.15. $C_{37}H_{46}N_6O_7$ requires C, 64.7; H, 6.75; N, 12.25%); ν/cm^{-1} 3115 (C–H), 2240 (C≡N), 1640 (C=O, amide), 1545 (NO_2) and 1350 (NO_2).

N,N-Didecyl-2,5,7-trinitro-9-dicyanomethylenefluorene-4-carboxamide 1l

2,5,7-Trinitro-9-oxofluorene-4-carboxylic acid[50] (20.0 g, 56 mmol), thionyl chloride (100 cm^3) and DMF (3 drops) were refluxed for 1 h. Excess thionyl chloride was removed under reduced pressure and the residue was dissolved in dry dioxane (150 cm^3). Decylamine (8.8 g, 56 mmol) and triethylamine (7.8 ml, 56 mmol) were added to this solution, the mixture was stirred for 1 h and poured into water (600 cm^3). A yellow-brown solid was collected and washed with water yielding *N,N*-didecyl-2,5,7-trinitro-9-oxofluorene-4-carboxamide (26.9 g, 97%), mp 216.5–218 °C (from acetonitrile) (Found: C, 58.1; H, 5.25; N, 11.25. $C_{24}H_{26}N_4O_8$ requires C, 57.8; H, 5.25; N, 11.25%); ν/cm^{-1} 3350 (N–H), 3120, 3095 (C–H), 1750 (C=O, fluorenone), 1645 (C=O, amide), 1550 (NO_2) and 1355 (NO_2).

The above amide (17.5 g, 35 mmol) and malononitrile (6.0 g, 91 mmol) were stirred in DMF (110 cm^3) at room temperature for 2.5 h. The solution was diluted with ethanol (300 cm^3) and

after 3 h the solid was filtered and washed with ethanol yielding amide **11** (18.7 g, 97.5%), mp 242–245 °C. Purification by column chromatography (3.5 × 8 cm) on silica gel (100–400 mesh) with benzene as eluent yielded **11** (16.2 g, 86.5%), mp 244–245 °C (Found: C, 59.25; H, 4.75; N, 15.45. $C_{27}H_{26}N_6O_7$ requires C, 59.35; H, 4.8; N, 15.4%); ν/cm^{-1} 3345 (N–H), 3245 (N–H), 3100 (C–H), 2240 (C≡N), 1650 (C=O, amide), 1545 (NO_2) and 1350 (NO_2).

2,4,5,7-Tetranitrofluoren-9-one 4

This compound was obtained as described previously,[51] mp 253–254 °C.

2,4,7-Trinitro- and 2,4,5,7-tetranitro-9-dimethylamino-methylenefluorenes 10a and 10b

These compounds were obtained by condensation of 2,4,7-trinitro-[52] and 2,4,5,7-tetranitro-fluorenes,[51] respectively, with dimethylformamide in acetic anhydride as described previously.[40]

2-Dimethylamino-4,5,7-trinitrofluoren-9-one 5

This compound was obtained by heating **4** with 33% aqueous dimethylamine in acetonitrile at 80 °C for 30 min; mp 271–273 °C (from acetonitrile)§§ (Found: C, 50.2; H, 2.8; N, 15.7. $C_{15}H_{10}N_4O_7$ requires C, 50.3; H, 2.8; N, 15.65%); δ_H([$^2H_6$]-acetone, Me_4Si) 8.83 (1 H, d, $J_{6,8}$ 2.1, 6-H), 8.53 (1 H, d, 8-H), 7.42 (1 H, d, $J_{1,3}$ 2.6, 3-H), 7.37 (1 H, d, 1-H) and 3.35 (6 H, s, NMe_2).

2,4,5-Trinitro-7-dimethylamino-9-dicyanomethylenefluorene 6

2.4,5-Trinitro-7-dimethylaminofluoren-9-one **5** (4.0 g, 11 mmol) was dissolved in DMF (70 cm^3) with heating up to 60 °C, malononitrile (1.52 g, 23 mmol) was added and the solution was stirred for 4 h at 75–80 °C. The mixture was diluted with propan-2-ol (300 cm^3), cooled and the dark solid was collected by filtration and washed with propan-2-ol, yielding **6** (4.16 g, 91.7%), mp 260–264 °C. After recrystallization by dissolving in dioxane (100 cm^3) and subsequent dilution with propan-2-ol (300 cm^3), dark violet crystals of **6** (3.15 g, 69.4%) were obtained, mp 266.5–268.5 °C (Found: C, 53.1; H, 2.6; N, 20.7. $C_{18}H_{10}N_6O_6$ requires C, 53.2; H, 2.5; N, 20.7%); δ_H([$^2H_6$]acetone, Me_4Si) 9.45 (1 H, d, $J_{1,3}$ 2.0, 1-H), 8.85 (1 H, d, 3-H), 8.13 (1 H, d, $J_{6,8}$ 2.5, 8-H), 7.46 (1 H, d, 6-H) and 3.35 (6 H, s, NMe_2).

2,7-Dinitro-4,5-X,Y-9-[cyano(dialkylamino)methylene]fluorene 2a–l. General procedure

2,7-Dinitro-4,5-X,Y-9-dicyanomethylenefluorene (**1**) was dissolved in dioxane or acetonitrile with heating up to 50–60 °C, the corresponding amine (1.0–1.1 equiv.) was then added and the mixture was stirred for 1–6 h at room temperature with monitoring of the reaction by TLC on silica gel [toluene–dioxane, 1:(4–6) v/v]. If the product crystallized, it was filtered off, washed with the same solvent and recrystallized for purification from the appropriate solvent as indicated in Table 1. In other cases, the reaction mixture was evaporated under reduced pressure and the residue was purified by column chromatography on silica gel (100–160 mesh) followed by recrystallization of the product when necessary (see Table 1). Conditions for the syntheses, yields and melting points of the products are summarized in Table 1.

2,7-Dinitro-4,5-X,Y-9-[bis(dialkylamino)methylene]fluorene 3a–g,i–k. General procedure

2,7-Dinitro-4,5-X,Y-9-dicyanomethylenefluorene **1** was dissolved in dioxane, acetonitrile or acetone with heating up to 50–60 °C, the corresponding amine (3–9 equiv.) was added and the mixture was stirred for 2–48 h at 25–55 °C with monitoring of the reaction by TLC on silica gel [toluene–dioxane, 1:(4–6) v/v]. Compounds **3f, i, j** and **k** were isolated by filtration (after cooling the reaction mixture) and purified by recrystallization from appropriate solvents. In other cases, the reaction mixture was evaporated under reduced pressure and the residue was purified by column chromatography on silica gel (100–160 mesh) followed by recrystallization of the product as indicated (see Table 1). Conditions for the syntheses, yields and melting points of the products are summarized in Table 1.

2,4,7-Trinitro-9-[dimethylamino(morpholino)methylene]-fluorene 3m

2,4,7-Trinitro-9-[cyano(morpholino)methylene]fluorene **2k** (2.5 g, 5.9 mmol) was dissolved in acetonitrile (900 cm^3) with heating, 33% aqueous dimethylamine (4.0 cm^3, 27 mmol) was added and the mixture was stirred for 2 h at room temperature. After evaporation of the solvent, crude **3m** (2.6 g, 99.7%) was isolated, mp 233–238 °C. After two recrystallizations from acetone, a dark violet crystalline product **3m** was obtained, mp 242–244 °C.

Kinetic measurements

The kinetics of the reaction **2i**→**3n** were studied spectrophotometrically by the decrease of the optical density of the initial substrate at 253, 435 and 527 nm under pseudo-first-order conditions (excess of amine). A SF-26 spectrophotometer (LOMO, USSR) connected with a 5-digital voltmeter model B7-17 was used with thermostatted (25 ± 0.2 °C) 1.00 cm silica cells. The kinetic method has been described previously.[53] Acetonitrile for kinetic measurements was purified as described earlier.[54]

Electrochemical measurements

Cyclic voltammetry experiments were performed on a EG & G PARC model 273 potentiostat with an Advanced Bryans XY recorder with iR compensation. Platinum wire, platinum disk (diameter 1.6 mm, BAS) and Ag/AgCl in acetonitrile were used as counter, working and reference electrodes, respectively. The ferrocene–ferrocenium couple was used as internal reference and potentials were calculated *versus* Ag/AgCl. Under our conditions the Fc^0/Fc^+ couple showed a potential of +0.45 V *vs.* Ag/AgCl.

In all the cases CV experiments were performed in dry acetonitrile (Fluka, anhydrous) with $Et_4N^+BF_4^-$ (Fluka, puriss) as supporting electrolyte (0.2 mol dm^{-3}) under N_2 flow, concentrations of acceptors were *ca.* 10^{-4} mol dm^{-3} and the scan can rate was 100 mV s^{-1}.

Spectroelectrochemical measurements

Spectroelectrochemistry was undertaken using a Perkin-Elmer Lambda 19 UV–VIS–near IR spectrophotometer with a Ministat (Thomson Electrochem Ltd, Newcastle upon Tyne, UK). The spectroelectrochemical cell was based on a 1 cm thick cuvette; Pt wire was used as a counter electrode, while Ag wire served as a quasi-reference electrode (all potentials were corrected to Ag/AgCl). A thin layer working electrode was constructed from glass and indium tin oxide conducting glass (sheet resistance is 30 Ω per square, from Balzers) held together with 0.1 mm thick polyether spacer (from Goodfellow) by Araldyte.

X-Ray single crystal structure determination for 2i

A dark purple single crystal of **2i** of dimensions 0.22 × 0.33 × 0.40 mm, grown from dioxane solution, was used for the X-ray diffraction experiment, performed on a Rigaku AFC6S four-circle diffractometer (graphite-monochromated Mo-Kα radiation, λ = 0.710 73 Å, 2θ–ω scan mode, $2\theta \leqslant 54°$, 3835 independent reflections measured, no absorption correction) at 150 K.

Crystal data. $C_{17}H_{10}N_6O_8$; M = 426.3; monoclinic; space

§§ This compound was synthesized by Dr A. M. Andrievskii and we are grateful to him for providing this compound.

group $C2/c$; a = 19.313(6), b = 10.680(3), c = 17.036(5) Å; β = 98.48(3)°; U = 3475(2) Å^3 (from 25 reflections with 13 < θ < 14°); Z = 8; $F(000)$ = 1744; D_c = 1.630 g cm^{-3}; absorption coefficient = 1.33 cm^{-1}.

The structure was solved by direct methods[55] and refined by full-matrix least-squares against Fs of 2196 reflections having $F \geqslant 4\sigma(F)$, with $w = [\sigma^2(F) + 0.0002\ F^2]^{-1}$ weights, using SHELXTL PLUS software.[56] All non-hydrogen atoms were refined with anisotropic displacement parameters and all H atoms in isotropic approximation (total of 322 variables), converging at R = 0.047, R_w = 0.048 and goodness-of-fit 1.33, residual electron density $\Delta\rho_{max}$ = 0.26, $\Delta\rho_{min}$ = −0.24 e Å^{-3}.

Additional material, comprising atomic coordinates, thermal parameters, bond lengths and angles, anisotropic and isotropic displacement coefficients, is available from the Cambridge Crystallographic Data Centre, reference code YILFII.¶¶

Photophysical measurements of PEPC films sensitized by fluorene acceptors

Photothermoplastic storage media were made by the following method: anionic PEPC (0.5 g) and a corresponding quantity of an acceptor were dissolved separately in toluene (both in 5 cm^3). The solutions were combined and filtered off. The resulting solution was cast onto a glass base with an electroconductive SnO_2 layer. The final thickness of the photosensitive films was 1.0–1.2 μm.

Measurements of photosensitivity of the photothermoplastic films were carried out at wavelengths over the range 400 to 900 nm. The charge potential of the surface of the films in the dark, made by a positive corona charge grid, was measured by dynamic sonde method. Dark decay of the surface potential measured for the time of 30 s was to be 10–15% of the initial potential. Electrophotographic sensitivity ($S_{\Delta V}$, m^2 J^{-1}) was estimated on the level of 20% decay of the initial potential under the illumination of 400 to 900 nm with the intensity of 0.1 μW cm^{-1}.

Acknowledgements

We thank the Royal Society (I. F. P. and L. M. G.), the University of Durham (L. M. G.) and EPSRC (A. S. B.) for financial support. M. R. B. thanks the University of Durham for a Sir Derman Christopherson Research Fellowship.

¶¶ For details of the deposition scheme, see 'Instructions for Authors', *J. Chem. Soc., Perkin Trans. 2*, 1996, Issue 1. Any request to the CCDC for this material should quote the full literature citation and reference number.

References

1 (*a*) Preliminary communication see: I. F. Perepichka, A. F. Popov, T. V. Artyomova, A. N. Vdovichenko, M. R. Bryce, A. S. Batsanov, J. A. K. Howard and (in part) J. L. Megson, *J. Chem. Soc., Perkin Trans. 2*, 1995, 3; (*b*) Part 4, D. D. Mysyk, I. F. Perepichka, A. S. Edzina and O. Ya. Neilands, *Latvian J. Chem.*, 1991, 727.
2 M. Matsui, K. Fukuyasu, K. Shibata and H. Muramatsu, *J. Chem. Soc., Perkin Trans. 2*, 1993, 1107; H. Hoegl, G. Barchietto, and D. Tar, *Photochem. Photobiol.*, 1972, **16**, 335.
3 N. G. Kuvshinsky, N. G. Nakhodkin, N. A. Davidenko, A. M. Belonozhko and D. D. Mysyk, *Ukr. Fiz. Zh.*, 1989, **34**, 1100 (*Phys. Abstr.*, 1989, **92**, 142486); N. M. Semenenko, V. N. Abramov, N. V. Kravchenko, V. S. Trushina, P. G. Buyanovskaya, V. L. Kashina and I. V. Mashkevich; *Zh. Obshch. Khim.*, 1985, **55**, 324 (*Chem. Abstr.*, 1985, **103**, 53782h).
4 V. E. Kampars and O. Ya. Neilands, *Usp. Khim.*, 1977, **46**, 945 (*Chem. Abstr.*, 1977, **87**, 101429y).
5 W. R. Hertler, H. D. Hartzler, D. S. Acker and R. E. Benson, *J. Am. Chem. Soc.*, 1962, **84**, 3387; B. C. McKusick, R. E. Heckert, T. L. Cairus, D. D. Coffman and H. F. Mower, *J. Am. Chem. Soc.*, 1958, **80**, 2806.
6 B. P. Bespalov and G. A. Tashbayev, *Zh. Org. Khim.*, 1980, **16**, 843 (*Chem. Abstr.*, 1980, **93**, 114180j).
7 L. A. Chetkina, Z. P. Povetyeva, V. K. Bel'skii and B. P. Bespalov, *Kristallografiya*, 1985, **30**, 910 (*Chem. Abstr.*, 1985, **103**, 204122w).
8 O. V. Semidetko, L. A. Chetkina, V. K. Bel'skii, D. D. Mysyk, I. F. Perepichka and A. M. Andrievskii, *Zh. Obshch. Khim.*, 1987, **57**, 415 (*Chem. Abstr.*, 1988, **108**, 204311k); A. M. Andrievskii, N. G. Grekhova, N. A. Andronova, R. R. Shifrina, V. N. Alexandrov and K. M. Dyumaev, *Zh. Org. Khim.*, 1982, **18**, 1961 (*Chem. Abstr.*, 1983, **98**, 106926v).
9 O. V. Chelysheva, L. A. Chetkina, V. K. Bel'skii and A. M. Andrievskii, *Kristallografiya*, 1989, **34**, 1020 (*Chem. Abstr.*, 1989, **111**, 164649e).
10 I. F. Perepichka, A. F. Popov, T. V. Orekhova, M. R. Bryce, A. S. Batsanov, A. M. Andrievskii, J. N. Heaton and J. A. K. Howard, unpublished results.
11 S. Hoz and D. Speizman, *J. Org. Chem.*, 1983, **48**, 2904.
12 T. K. Mukherjee and L. A. Levasseur, *J. Org. Chem.*, 1965, **30**, 622.
13 (*a*) Z. Rappoport, *Acc. Chem. Res.*, 1981, **14**, 7 and references cited therein; (*b*) H. Shenhav, Z. Rappoport and S. Patai, *J. Chem. Soc. B*, 1970, 469; (c) Z. Rappoport and A. Topol, *J. Chem. Soc., Perkin Trans. 2*, 1975, 863; (d) Z. Rappoport and D. Ladkani, *Chem Scri.*, 1974, **5**, 124.
14 Z. Rappoport, *Adv. Phys. Org. Chem.*, 1969, **7**, 1; G. Modena, *Acc. Chem. Res.*, 1971, **4**, 73.
15 G. Modena, P. E. Todesco, and S. Tonti, *Gazz. Chim. Ital.*, 1959, **89**, 878; G. Modena, F. Taddei, and P. E. Todesco, *Ric. Sci.*, 1960, **30**, 894; L. Maioli, G. Modena, and P. E. Todesco, *Bol. Sci. Fac. Chim. Ind. Bologna*, 1960, **18**, 66 (*Chem. Abstr.*, 1962, **56**, 5872g); A. Campagni, G. Modena, and P. E. Todesco, *Gazz. Chim. Ital.*, 1960, **90**, 694; F. Scotti and E. J. Frazza, *J. Org. Chem.*, 1964, **29**, 1800; F. Beltrame, G. Favini, M. G. Cattania and F. Guella, *Gazz. Chim. Ital.*, 1968, **98**, 380; Z. Rappoport and A. Topol, *J. Chem. Soc., Perkin Trans. 2*, 1975, 982.
16 (*a*) Z. Rappoport and R. Ta-Shma, *J. Chem. Soc. B*, 1971, 871; (*b*) Z. Rappoport and R. Ta-Shma, *J. Chem. Soc. B*, 1971, 1461; (*c*) Z. Rappoport and N. Ronen, *J. Chem. Soc., Perkin Trans. 2*, 1972, 955.
17 Z. Rappoport and P. Peled, *J. Chem. Soc., Perkin Trans. 2*, 1973, 616.
18 Z. Rappoport and D. Ladkani, *J. Chem. Soc., Perkin Trans. 2*, 1973, 1045.
19 L. Pauling, *The Nature of the Chemical Bond*, Cornell University Press, Ithaca, 1960, p. 232.
20 D. Adhikesavalu and K. Venkatesan, *Acta Crystallogr., Sect. C*, 1983, **39**, 589.
21 B. Tinant, J.-P. Declerq, D. Bouvy, Z. Janousek and H. G. Viehe, *J. Chem. Soc., Perkins Trans. 2*, 1993, 911.
22 F. H. Allen, O. Kennard, D. G. Watson, L. Brammer, A. G. Orpen and R. Taylor, *J. Chem. Soc., Perkin Trans. 2*, 1987, S1.
23 B. Beaglay, *Molecular Structure by Diffraction Methods*, 1973, vol. 1, p. 59.
24 Y. Morino, K. Kuchitsu, T. Fukuyama and M. Tanimoto, *Acta Crystallogr., Sect. A*, 1969, **25**, S127.
25 A. Gavezzotti, *J. Am. Chem. Soc.*, 1983, **105**, 5220.
26 J. Silverman, N. F. Yannoni and A. P. Krukonis, *Acta Crystallogr., Sect. B*, 1974, **30**, 1474.
27 O. V. Semidetko, L. A. Chetkina, V. K. Bel'skii, A. N. Poplavskii, A. M. Andrievskii and K. M. Dyumaev, *Zh. Strukt. Khim.*, 1988, **29**, 187 (*Chem. Abs.*, 1988, **109**, 139617u).
28 O. V. Semidetko, L. A. Chetkina, V. K. Bel'skii, A. N. Poplavskii, A. M. Andrievskii and K. M. Dyumaev, *Dokl. Akad. Nauk SSSR*, 1988, **299**, 375 (*Chem. Abstr.*, 1989, **111**, 96782r).
29 L. A. Chetkina, O. V. Semidetko, V. K. Bels'kii, A. N. Sobolev and A. M. Andrievskii, *Acta Crystallogr., Sect. C*, 1987, **43**, 933.
30 R. G. Baughman, *Acta Crystallogr., Sect. C*, 1987, **43**, 931.
31 J. Silverman and N. F. Yannoni, *J. Phys. Chem.*, 1967, **71**, 1381.
32 S. V. Nyburg and C. H. Fraerman, *Acta Crystallogr., Sect. B*, 1985, **41**, 274.
33 R. R. Gagné, C. A. Koval and G. C. Lisensky, *Inorg. Chem.*, 1980, **19**, 2854; G. Gritzner and J. Kuta, *Pure Appl. Chem.*, 1982, **54**, 1527; G. Gritzner and J. Kuta, *Pure Appl. Chem.*, 1984, **56**, 461; A. M. Bond, E. A. McLennan, R. S. Stojanovic and F. G. Thomas, *Anal. Chem.*, 1987, **59**, 2853.
34 B. S. Jensen, V. D. Parker, *J. Am. Chem. Soc.*, 1975, **97**, 5211; A. Rainis and M. Szwarc, *J. Am. Chem. Soc.*, 1974, **96**, 3008.
35 S. Hünig, *Pure Appl. Chem.*, 1990, **62**, 395; K. Hesse and S. Hünig, *Liebigs Ann. Chem.*, 1985, 708, and references cited therein.
36 I. A. Koppel and V. A. Palm, in *Advances in Linear Free Energy Relationships*, eds. N. B. Chapman and J. Shorter, Plenum, London, 1972, ch. 5, p. 203; V. A. Palm, *Fundamentals of Quantitative Theory of Organic Reactions*, Khimiya, Leningrad, 1977, p. 109 (in Russian).

37 C. Hansch and A. J. Leo, *Substituent Constants for Correlation Analysis in Chemistry and Biology*, Wiley, New York, 1979.
38 *Handbook of the Properties of Organic Compounds*, ed. A. A. Potekhin, Khimiya, Leningrad, 1984, p. 79 (in Russian).
39 D. D. Mysyk and I. F. Perepichka, *Phosphorus, Sulfur, and Silicon*, 1994, **95–96**, 527.
40 N. V. Kravchenko, V. N. Abramov and N. M. Semenenko, *Zh. Org. Khim.*, 1989, **25**, 1938 (*Chem. Abstr.*, 1990, **112**, 178292r).
41 E. S. Amis, *Solvents Effects on Reaction Rate and Mechanism*, Academic Press, New York and London, 1966.
42 R. G. Makitra and Ya. N. Pirig, *Zh. Obhsch. Khim.*, 1986, **56**, 657 (*Chem. Abstr.*, 1987, **106**, 108682v).
43 D. D. Mysyk, I. F. Perepichka, V. E. Romashev, A. M. Andrievsky and L. I. Kostenko, USSRP 1 241 673/1984; D. D. Mysyk, I. F. Perepichka, N. M. Sivchenkova, L. I. Kostenko and V. E. Romashev, in *Organic Semiconducting Materials*, Perm' University, Perm', 1985, Issue 8, p. 108.
44 N. M. Semenenko, V. N. Abramov, N. V. Kravchenko, V. S. Trushina, N. G. Buyanovskaya, V. L. Kashina and I. V. Mashkevich, *Zh. Obshch. Khim.*, 1984, **55**, 324 (*Chem. Abstr.*, 1985, **103**, 53782h); V. N. Abramov, A. M. Andrievsky, N. A. Bodrova, M. S. Borodkina, N. V. Kravchenko, L. I. Kostenko, I. A. Malakhova, E. G. Nikitina, I. G. Orlov, I. F. Perepichka, I. S. Pototskii, N. M. Semenenko and V. S. Trushina, USSRP 1 343 760/1985.
45 A. J. Gordon and R. A. Ford, *The Chemist's Companion. A Handbook of Practical Data, Techniques, and References*, Wiley, New York, 1972.
46 T. K. Mukherjee, *Tetrahedron*, 1968, **24**, 721.
47 M. S. Bloom and C. F. Groner, *Res. Dis.*, 1977, **154**, 32 (*Chem. Abstr.*, 1977, **86**, 197870p).
48 D. D. Mysyk, I. F. Perepichka, N. M. Sivchenkova, V. E. Kampars, O. Ya. Neilands and R. B. Kampare, *Latv. PSR Zinat. Akad. Vestis. Kim. Ser.*, 1984, 328 (*Chem. Abstr.*, 1984, **101**, 210699q).
49 D. D. Mysyk, N. M. Sivchenkova, V. E. Kampars, and O. Ya. Neilands, *Latv. PSR Zinat. Akad. Vestis. Kim. Ser.*, 1987, 621 (*Chem. Abstr.*, 1988, **109**, 92406q).
50 G. I. Migachev, N. G. Grekhova and N. S. Dokunikhin, *Zh. Org. Khim.*, 1978, **14**, 2380 (*Chem. Abstr.*, 1979, **90**, 137550g).
51 I. F. Perepichka and D. D. Mysyk, USSRP 862 561/1981; D. D. Mysyk, I. F. Perepichka and L. I. Kostenko, USSRP 1 050 249/1983.
52 A. Yoshiro, *Nippon Kagaku Kaishi*, 1981, 1966.
53 I. F. Perepichka, L. I. Kostenko, A. F. Popov and A. Yu Chervinskii, *Zh. Org. Khim.*, 1988, **24**, 822 (*Chem. Abstr.*, 1989, **110**, 94216q); A. F. Popov, I. F. Perepichka and L. I. Kostenko, *J. Chem. Soc., Perkin Trans. 2*, 1989, 395.
54 L. I. Kostenko, A. F. Popov, V. V. Kravchenko and I. F. Perepichka, *Zh. Org. Khim.*, 1986, **22**, 245 (*Chem. Abstr.*, 1986, **105**, 42026e).
55 G. M. Sheldrick, *Acta Crystallogr., Sect. A*, 1990, **46**, 467.
56 G. M. Sheldrick, SHELXTL-PLUS, Göttingen and Siemens PLC, 1990.

Paper 6/01937D
Received 20*th March* 1996
Accepted 7*th June* 1996